GEOLOGICA BELGICA (2008) 12/1-2: 3-23

SEDIMENTOLOGICAL CONTROL ON CARBONATE CEMENTATION IN THE LUXEMBOURG SANDSTONE FORMATION

Koen VAN DEN BRIL & Rudy SWENNEN

(8 figures, 2 tables and 2 plates)

Department of Earth and Environmental Sciences, K.U. Leuven, Celestijnenlaan 200E, B-3001 Heverlee, Belgium.
E-mail: Koen.vandenbril@ees.kuleuven.be, Rudy.Swennen@ees.kuleuven.be

ABSTRACT. The Luxembourg Sandstone Formation, i.e. a lower Jurassic offshore sandbar complex which was deposited in a general transgressive regime, was studied with the aim to unravel the controlling parameters and variations on calcite cementation. This work was based on a combination of extensive fieldwork, petrographic and geochemical analyses. Cementation started with the development of acicular and equant cement. Both have been replaced in the meteoric realm by ferroan calcite cement. Elongated cemented lenses (10-100 m) are parallel to the bedding planes of cross-stratified layers. Coarse-grained cemented channels have a lensoid outline. Continuously cemented (>> 100 m) layers are present (1) as coarse-grained bioclastic rich layers in finer-grained lithologies (both sands and marls) and (2) at important lithological boundaries. Small nodules composed of sparitic to poikilotopic calcite cements, are aligned parallel to the stratification of the sandstones. The outline and distribution of the lenses is the result of an early cementation process, which affected carbonate-rich strata. Later diagenetic redistribution of unstable carbonate from the uncemented strata enhanced the early diagenetic signature. This resulted in zones containing a large amount of up to 100 m elongated lenses, zones with smaller (1–10 m) lenses and zones without any lenses.

KEYWORDS. Luxembourg Sandstone, Diagenesis, Calcite cementation

1. Introduction

Laterally extensive carbonate cementation in the form of concretions, lenses or continuous cemented layers is widely recognised in shallow-marine sandstones. In the late 80's and 90's, research focused on carbonate concretions in shallow marine sands. Knowledge on origin, distribution and geometry of carbonate cementation is of prime importance in reservoir characterisation, since this cementation may act as a barrier for fluid flow and can even lead to reservoir compartmentalisation (Gibbons *et al.*, 1993; Prosser *et al.*, 1993). Especially in the North Sea basin different Jurassic reservoir rocks bear this type of diagenetic alterations (Bjørlykke & Brensdal, 1986; Walderhaug *et al.*, 1989; Walderhaug & Bjørkum, 1992; Hendry *et al.*, 2000). A large number of publications hence deal with these reservoir heterogeneities and reservoir analogues from adjacent areas such as e.g. the Bridport Sands and the Valtos Formation (Kantorowicz *et al.*, 1987; Wilkinson, 1991; Bjørkum & Walderhaug, 1993; Wilkinson, 1993).

It is generally accepted that the distribution of these concretions is related to the presence of primary carbonate, which repartition is controlled by depositional environment. In order to improve the predictability, more recent studies incorporate diagenesis into a sequence stratigraphic framework (Taylor *et al.*, 1995; Morad *et al.*, 2000; Ketzer *et al.*, 2002; Al-Ramadam *et al.*, 2005, Burns *et al.*, 2005; El-ghali *et al.*, 2006).

In this contribution the Luxembourg Sandstone Formation is presented as a reservoir analogue to study the relationship between sedimentology and early diagenesis with respect to concretionary calcite cementation. The outcrops expose continuously calcite cemented mega-scale foresets, cemented channel-fill deposits and storm layers, hardground development and small-scale concretions along foresets, which thus allows to address stratigraphic or depositional controls.

2. Geological setting

The Luxembourg Sandstone Formation has been deposited during the Hettangian and Sinemurian in the Lorraine region of southern Belgium and northern France, and the Grand-Duchy of Luxembourg (Fig. 1). The diachronic nature of the sandstone has been clearly revealed by palaeontological research (Guerin-Franiatte & Muller, 1986; Guerin-Franiatte *et al.*, 1991) using ammonite biozones. Recently, the lithological changes in the Lorraine region of Belgium have been reinterpreted within a stratigraphic framework (Boulvain *et al.*, 2000, 2001). In Belgium, the formation is subdivided in different members, separated by marl horizons (Fig. 2). The sandbody is deposited as an offshore sand wave complex reflecting a general transgressive regime, which can be related to the onset of the Ligurian cycle in the Paris Basin (De Graciansky *et al.*, 1998a). This Jurassic transgression started from the German basin and reached the Paris Basin through the Luxembourg seaway (De Graciansky *et al.*, 1998b). The Hettangian - Lower Sinemurian transition is marked by a peak transgression which explains an important shift of the depocentre towards the Ardennes

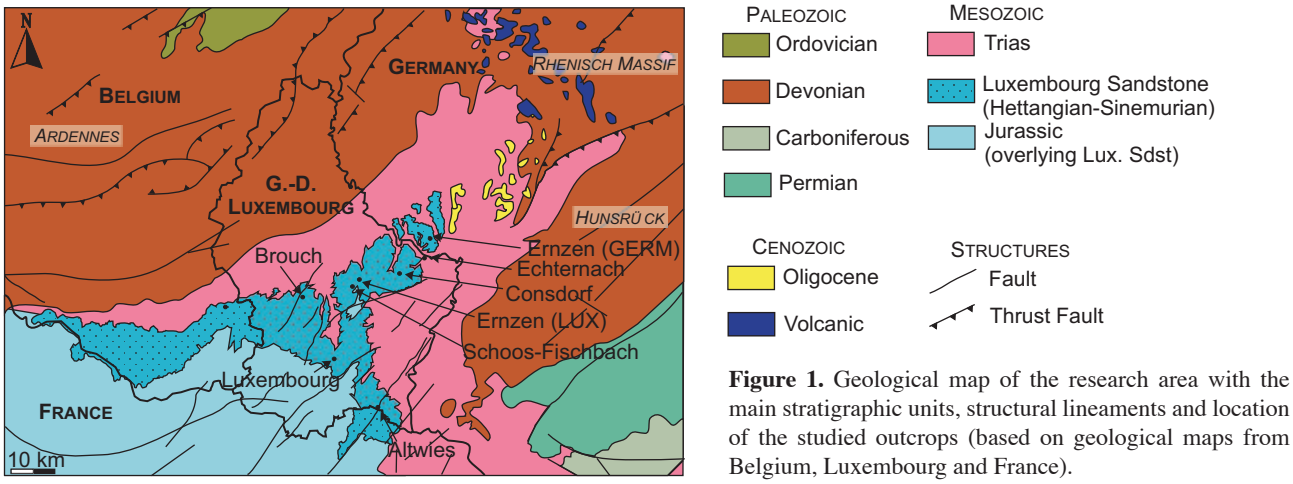

Figure 1. Geological map of the research area with the main stratigraphic units, structural lineaments and location of the studied outcrops (based on geological maps from Belgium, Luxembourg and France).

massif (Fig. 1). The Formation is embedded in marls. Marls and dolostones of the Levallois and Jamoigne Formations of Keuper to Hettangian age occur below the Luxembourg Sandstone Formation and the latter is overlain the Sinemurian Strassen Marls of the Arlon Formation (Fig. 2).

The sedimentological and paleogeographical setting of the Luxembourg Sandstone Formation has been described in detail by Monteyne (1967), Berners (1983, 1985) and Mertens *et al.* (1983). The formation generally consists of sand waves and bars that have been deposited in a tidal influenced deltaic environment. A normal "sequence" starts with low angle to fine laminated subtidally deposited sands, followed by large scale sand bars with mega foresets. The "sequence" is bounded by lag depositis, tidal channels and bidirectionally cross-stratified sands.

Structural control of the basement during deposition resulted in important and rapid thickness variations. The post-depositional evolution of the Luxembourg Sandstone Formation is related to the subsidence history of the Paris Basin (Guillocheau *et al.*, 2000). The latter is influenced by the rifting of the Tethys, the Mid Jurassic doming event in the North Sea, the formation of the Rhine Graben and the Alpine collision. The main faults in the Mesozoic cover have a NE direction (e.g. Luxembourg Fault). The direction of these faults is inherited from the Variscan basement below and they are interpreted to be reactivated as extensional faults during the Mesozoic as a result of the Tethyan rift.

A second fracture pattern in the Luxembourg Sandstone Formation is developed as small, discontinuous cracks on a regular decimetric distance in the cemented lenses and as large fractures cutting across the formation. The former are cemented as small veins. The main directions are N30E/NE-SW and NW-SE. In most instances no large displacements were observed along the fractures. They can be interpreted as tensile cracks or a joint pattern, which has formed during uplift event under the regional stress field.

3. Methods

The sands were studied in outcrops along roads and hiking trails, and in three quarries covering a depositional area from proximal to distal (Fig. 1). In total eight outcrops in Luxembourg and Germany were studied and graphic logs were made. Samples were taken from cemented lenses, i.e. continuous cemented layers in fine-grained sediments, cemented channel lags and storm layers, as well as from the non cemented material. Additionally well cores from the Consdorf borehole were studied and sampled, in an attempt to study subsurface, possibly unaltered rock material. The Brouch outcrop, which covers the transition of the Hettangian to Sinemurian, is presented as a representative case since it illustrates well the relationships between different facies types and the diagenetic alterations. This quarry has been sedimentologically studied in detail by Berners (1985).

In general, the lithology was described as cemented or uncemented sand and marls, with exception of the beds which clearly contained macroscopically more than 90 % carbonate fragments. The latter were classified as limestone beds. Grain size analyses were conducted on 40 samples after physical (disaggregation) and chemical (decalcification, removal of Fe oxides and organic matter) pre-treatment. The measurements were conducted by laser diffraction (Malvern Mastersizer, Malvern Instruments Ltd., Worcestershire, UK) and the results were analysed with gradistat v5.0 (Blott & Pye, 2001).

158 samples were impregnated with blue or yellow epoxy before thin section preparation to visualise porosity. Most thin sections were stained using a mixture of alizarin red and potassium ferricyanide. The latter allows to differentiate ferroan and non-ferroan dolomite and calcite phases. All thin sections were examined using standard polarised light microscopy as well as cold cathodoluminescence (Technosyn) to visualise cement zonations. Operating conditions were 10-14 kV gun potential, 200-350 µA beam current, 0.05 Torr vacuum and 5 mm beam width. 100 modal analyses of the sandstones were performed by counting 1000 points per thin section using an in house build point counting stage

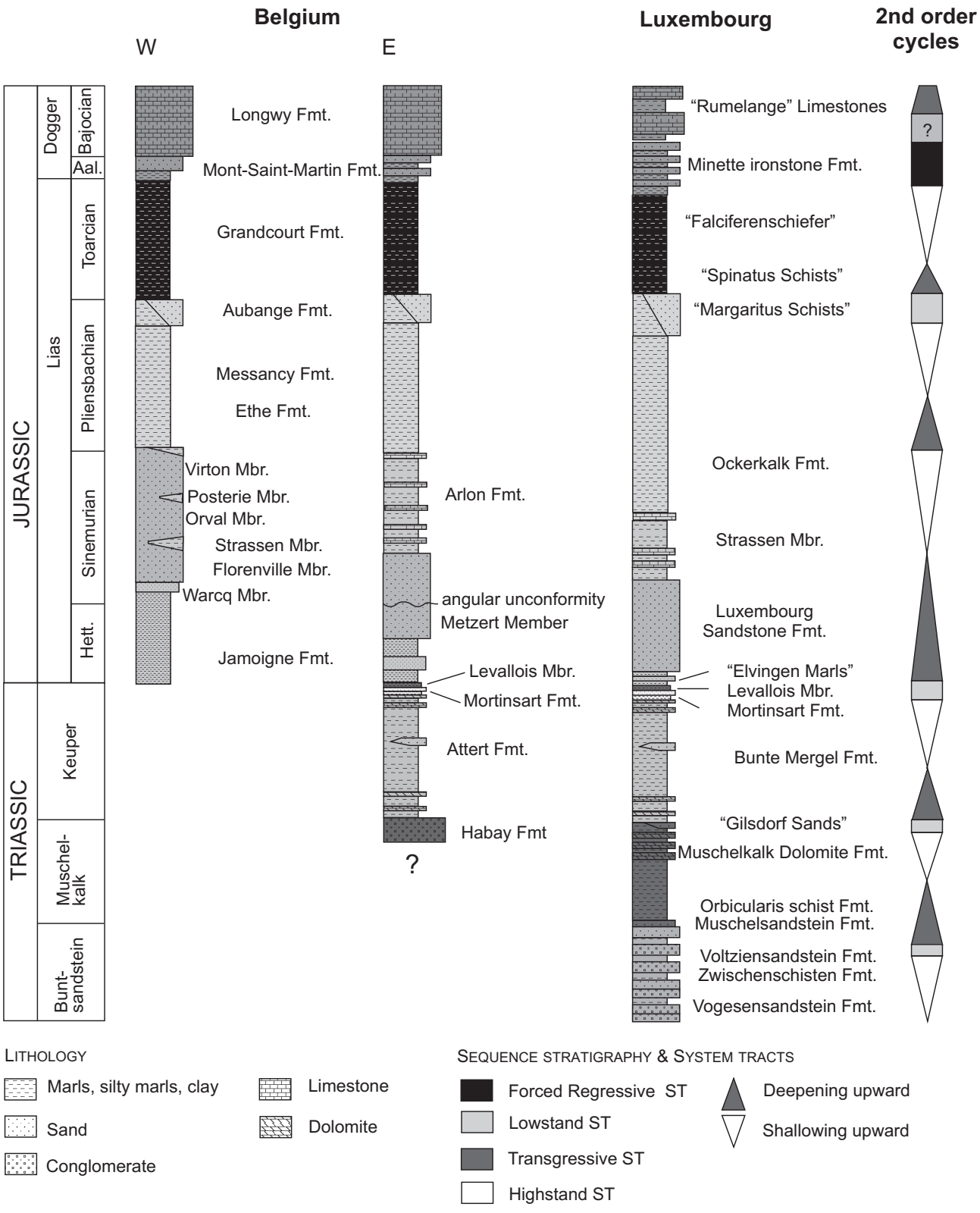

Figure 2. Lithostratigraphy of the Triassic and Lower Jurassic in Belgium (modified from Boulvain *et al*., 2000) and Luxembourg (compiled from Lucius, 1948; Service Geologique de Luxembourg) and tentative sequence stratigraphic interpretation (compiled from De Graciansky *et al*., 1998b; Hallam, 2001; Vecsei & Duringer, 2003; Bourquin *et al*., 2006)

Facies	Description	Interpretation/environment	Cementation pattern	Subfacies Berner (1985)
1	Homogeneous sands	Fast deposition	No cementation	Not described
2	Marls, bioturbated sandy marls and limestone beds	Open marine environment	Horizontal & continuous on outcrop scale	Lorraine Facies
3	Very fine grained sands	Lower shoreface sandsheets	Continuous and lenses	Initial sandbar facies
4	Cross-stratified sandstone beds	Middle shoreface tidal influenced sand waves	Lenses (up to 10 m)	Distal sandbar and inter sandbar facies
5	Large scale cross-stratified sandstone beds	Sand dunes	Elongated lenses (10 m)	Prograding sandbar
6	Bidirectional cross-stratified sands	Upper shoreface tidal influenced sand waves	Lenses (up to 5 m)	Sandbank facies
7	Low angle cross-stratified beds	Storm generated layers	Uncemented	Present in all facies
8	Coarse grained gravel layers	Storm layers/gravel lag deposits.	Continuously cemented on outcrop scale	Sandbank facies
9	Coarse grained gravel lenses	Tidal channels	Lensoid cementation (3 m and larger)	Sandbank facies
10	Encrusted layer	Hardground	Continuously cemented on outcrop scale	Special feature
11	Limestone marl alternation	Offshore marls and limestone beds. Climate controlled	Continuously cemented	Overlying lithology

Table 1: Facies description, interpretation and cementation geometry

controlled by a software made in excel. A Jeol JSM-6400 scanning electron microscope (SEM) equipped with an EDX analyser (Exl Link) was used to refine the paragenetic relationships.

Samples of the different calcite cements were taken for stable isotope analysis using a dental drill (Dremel). Several vein generations, recrystallised and original bioclasts could be sampled separately. Matrix cement however was bulk sampled. The analyses were conducted at the University of Erlangen in the Institute of Geology and Mineralogy. Carbonate powders were reacted with 100% phosphoric acid at 75°C using a Kiel III online carbonate preparation line connected to a ThermoFinnigan 252 masspectrometer. All values are reported in per mil relative to V-PDB by assigning a $\delta^{13}C$ value of +1.95‰ and a $\delta^{18}O$ value of -2.20‰ to NBS19. Reproducibility was checked by replicate analysis of laboratory standards and is better than ± 0.05 (1σ).

4. Sandstone facies

The sedimentary architecture is composed different facies. Originally, a sequence of the prograding sandbar complex was subdivided into 6 subfacies, namely: (1) Lorraine facies, (2) initial sandbar facies, (3) inter sandbar facies, (4) distal sand bar facies, (5) proximal sandbar facies and (6) sand bank facies (Berners, 1985). However in this study, based on a thorough description (and loss from interpretation), 11 facies have been distinguished. Obviously, the latter can be related to the original subdivision. The lithofacies and their interpretation within the depositional model of Berners (1985) are summarised in Table 1 and their occurrence in the Brouch section is shown in Figs 3 and 4.

4.1. Facies 1: Homogeneous sands

Description

The base of the Luxembourg Sandstone Formation is at several locations characterised by homogeneous medium to fine moderately well-sorted uncemented sandstones with bed thickness of 1 m. The observed total thickness of this facies generally is approximately 2 to 5 m. There are some clay drapes and locally 30 cm thick bioturbated horizons occur.

Interpretation

The occurrence of homogeneous sandstones may indicate fast deposition, with some periods of non deposition during which sediments were bioturbated and small millimetre scale clay laminae were deposited. As this facies occurs at the base of the formation, it is related to a transgressive pulse, which causes input of clastic terrigenious material.

4.2. Facies 2: Marls, bioturbated sandy marls and limestone beds

Description

This heterolithic facies consists of an alternation of laminated marls, bioturbated sandy marls and thin (cm scale) limestone beds. The sediments are poorly-sorted. The laminated marls are generally uncemented, whereas thin limestone beds are laterally continuously cemented.

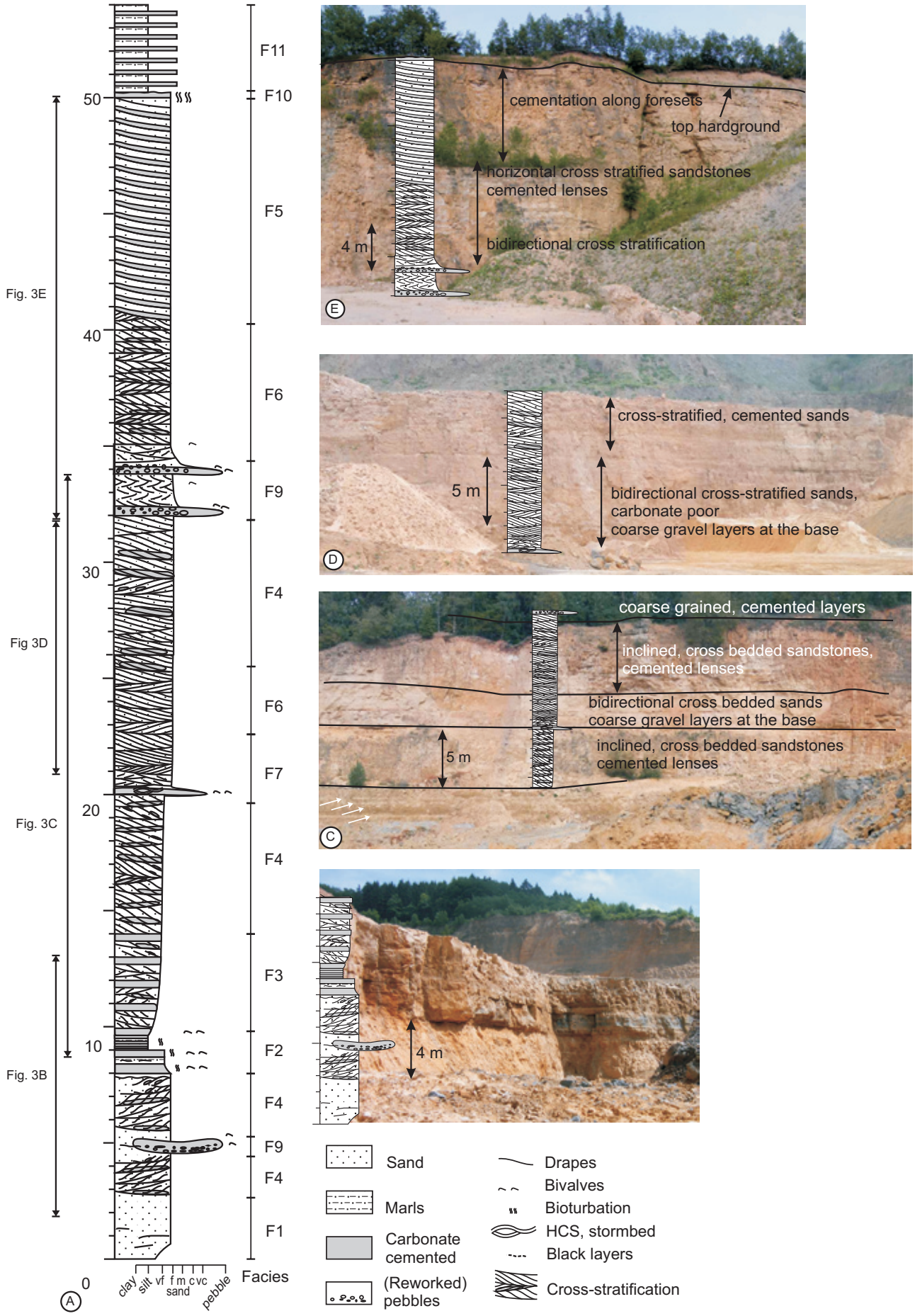

Figure 3. (A) Sedimentary log of the Brouch section with location of the different facies (for explanation see text) and (B-E) photographs of some representative field sections.

The base of these beds is sometimes slightly erosive. The beds are composed of coarse-grained bioclastic material such as bivalve shell fragments. The beds are overlain by laminated marls. Bioturbated sandy marls are characterised by a cruziana ichnofabric and tend to be continuously cemented.

Interpretation

The presence of the fine-grained sediments suggests deposition in offshore environments below wave base. Bioturbated layers are generally composed of somewhat coarser sediment, implying more shallow conditions or variable input of more sandy sediments. The bioturbated intervals suggests periods of low sediment influx. The erosive coarse-grained limestone beds can be related to storm events (e.g. Aigner, 1985).

4.3. Facies 3: Very fine-grained sands

Description

The very fine-grained (< 125 µm) sands are characterised by horizontal flaser bedding, ripples, thin (to 20 cm) cross-stratified beds and bioturbated zones. The sands generally have a high clay content and organic material occurs along the laminations. Thin (5 cm) continuous limestone beds can be found. Cemented sands are present as horizontal layers and smaller lenses. The cemented layers correspond to coarser-grained, skeletal limestone beds or bioturbated beds.

Interpretation

This facies can be interpreted as sand sheets, which have been deposited at the lower shoreface and offshore transition zone. During periods of no deposition, the deposited sands became bioturbated. The ichnofacies in calmer depositional environments are dominated by the Cruziana trace fossil assemblage (Hary & Muller, 1993). The limestone beds can be related to storm activity.

4.4. Facies 4: Cross-stratified sandstone beds

Description

This facies consists of fine- to medium-grained moderately well-sorted sands. Different patterns of cross-stratification can be identified. In the description below, the classification from Allen (1963) was used. The cross-stratified sandstone beds can be grouped in cosets, which are separated from the other sedimentary units by erosion surfaces. The dip direction (SW) of the stratification varies and thinner beds with an opposed set-direction (NE) exist. The magnitude of the cross-stratified sandstone beds is generally of decimetre scale (i.e. from 30 to 90 cm). Both planar and irregular lower bounding surfaces occur. The latter are sometimes slightly undulating. The bounding surfaces generally are reactivation surfaces. Within the beds some higher order reactivation surfaces occur. Bottomsets, if present, are marked by thin clay laminae and show bioturbation. Clay drapes are locally present along the foreset laminae.

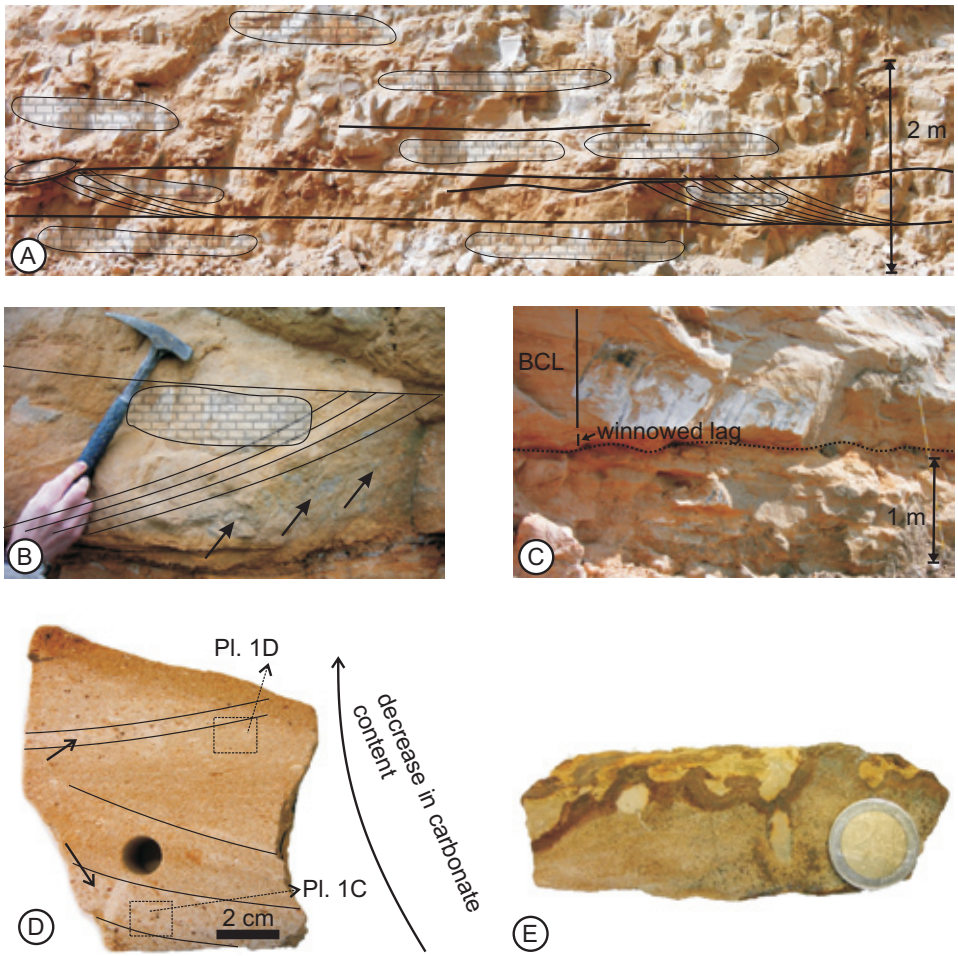

Figure 4. Field photographs: (A) Cemented lenses in the cross-stratified sandstones of facies type 4. The base of the beds is often undulating and within the layers, small scale reactivation surfaces occur. The cross-stratification indicates that directions of migration varied. (B) Small cemented lens at the top of cross-stratified sands below which several nodular cemented lenses occur along the foresets (see arrow). (C) Erosive contact (dashed line) on top of the cross-stratified sand facies, overlain by a 10 cm thick winnowed lag deposit which is interpreted as a storm layer. BCL: Bidirectional trough cross-stratified sands. (D) Cut surface from sample taken from a coarse grained bioclast rich layers. Stratification laminae are marked by the solid lines, zones with coarse grained bioclastic material are indicated by the arrows. Locations of thin section are marked by the dashed squares. (E) Hand specimen of the encrusted and bioturbated cemented layer on top of the Luxembourg Sandstone.

Within the cross-stratified sandstone beds cemented lenses regularly occur (Fig. 4A). They are bounded at the base by reactivation surfaces and clay drapes along the foreset laminae. The stratification generally has been preserved in the cemented lenses. Locally, small nodular calcite cemented geometries are observed along the stratification laminae of the cross-stratified beds (Fig. 4B).

Interpretation

Based on the presence of reactivation surfaces, clay drapes along the foreset laminae and presence of layers with cross-stratified dip direction opposed to the main dip direction, the cross-stratified sandstone layers can be interpreted as different classes of tidal influenced sand waves (Allen, 1980). The type of cross-stratified bed is determined by the influence of reversing current, which will be higher in beds with higher order reactivation surfaces.

4.5. Facies 5: Large scale cross-stratified sandstone beds

Description

This facies is characterised by large scale (up to several metres) cross-stratified fine to medium-grained well-sorted sand bodies. These sand bodies are very continuous and their dip tangential on a planar lower bounding surface. Although not observed in every location, carbonate cementation occurs as elongated lenses along the stratification (Fig. 3E).

Interpretation

The structures expressed in this facies can be interpreted as solitary submarine sand dunes, which are characterised by a high asymmetrical form, resulting from strong unidirectional currents. They can be interpreted as lateral transition of gently dipping compound sets (Allen, 1984; Johnson & Baldwin, 1986). These large dunes are however less frequently observed.

4.6. Facies 6: Bidirectional cross-stratified sands

Description

This facies is characterised by 10 to 30 cm thick bidirectional cross-stratified fine to medium-grained well-sorted sand beds, which can be grouped in cosets with a thickness up to several metres. Their lower bounding surfaces are planar to trough-shaped. The beds are separated from each other by reactivation surfaces and within the beds generally higher order reactivation surfaces occur. These are generally marked by clay drapes.

Calcite cemented zones normally occur as lenses of variable length. However, overall presence of calcite lenses is less than in the cross stratified beds of facies 4.

Interpretation

This facies is related to facies 4. It is composed of tidal influenced sand waves, but with more influence of alternating current directions resulting in bidirectional cross-stratification and trough-shaped sets. They represent more shallow marine conditions close to the mean low tide water level.

4.7. Facies 7: Storm beds.

Description

In the marls and very fine grained sands, different wavy and low angle cross-stratified sandbeds were recognised. Within the cross-stratified sandstone beds of facies 4, thicker units of relative coarser grained sand waves are present (Fig 4C). The thickness of these beds varies from centimetre (in low energy environments) to metre scale (in higher energy environments). Below these beds an erosive surface and thin lag deposit is usually present. The winnowed lags are enriched in coarse carbonate fragments and the overlying beds are generally carbonate poor and consist of medium to coarse-grained sands.

Interpretation

This facies can occur at different levels of the sedimentary sequences and indicates storm events. The facies show proximality trends (Aigner, 1985). In laminated marls from distal environments below the storm wave base, storm layers are indicated by deposition of a thin HCS bed. In more proximal environments, the deposition high energy dunes above an erosion surfaces and winnowed pebble lag is more pronounced (Anderton, 1976).

4.8. Facies 8: Coarse-grained bioclastic gravel layers

Description

This facies is continuous on outcrop scale. The layers generally have an irregular erosive base (Fig. 4C) with incisions up to 5 m deep. Although the thickness is variable, a distinction can be made between layers of approximately 10 cm thick and layers with thicknesses of 30 cm or more. Obviously, near the incisions their thickness increases in function of the depth of incisions. Lithologically they are composed of quartzite pebbles, well rounded calcite cemented clasts (with diameter up to 20 cm) and bioclasts. They display a fining upward trend. The sedimentary composition varies laterally. Some layers are well cemented whereas others are not. The latter are only composed of sand and quartzite pebbles. Above the coarse-grained layers, generally the sands of facies 6 or 7 occur. In bioclast-rich zones, some stratification was observed. Coarse-grained stratification laminae are enriched in bioclasts (echinoderm fragments & bivalve shells) whereas the finer-grained stratification laminae are more sand rich zones (Fig. 4D). This illustrates sorting of the sands on a very small scale.

Interpretation

The generation of thicker coarse-grained gravel layers with high amount of calcite cemented pebbles, quartzite pebbles and coarse bioclastic fragments indicates shallow marine conditions where reworking of the previously deposited material occurs as suggested by the presence of calcite cemented clasts. This reworking might have been associated with lateral erosional shifts in the deposition area (Mertens et al., 1983). Where currents were strongly localised, deep incisions could develop such as recognised in estuarial environments (Boersma & Terwindt, 1981).

Thinner coarse-grained beds can be produced during storms by washing out the finer grains and accumulation

of the heavier pebbles. The storm generated layers generally show the characteristics of proximal storm layers (Aigner, 1985) and are thus closely related with higher energy environments.

4.9. Facies 9: Local coarse-grained bioclastic gravel bodies

Description

This lithology corresponds to that of the coarse-grained layers, with clasts and shell debris at the base and sands near the top. The facies occurs as local cemented bodies. Their thickness varies from 50 cm up to more than 1 m. The base of these bodies is erosive and cuts into the underlying sands. The observed lateral extension is variable from 3 to 5 m.

Interpretation

These bodies can be interpreted as small channels which have been filled with coarse-grained material. The channels have formed by localised currents, probably as tidal channels.

4.10. Facies 10: Encrusted sandstone

Description

This facies is systematically found on top of a sandstone sequence underlying the Marls of Strassen. It generally consists of a well cemented sandstone layer (10 to 20 cm thickness), characterised by cm scale encrustations (Fig. 4F) and perforations. The encrustations have been refilled with fine-grained material and pyrite.

Interpretation

Encrusted sandstones can be interpreted as a hardground, which in contrast with other bioturbated zones shows clear evidence of borings in the cemented substratum. In combination with the overlying marls (facies 11), the hardground might be interpreted as a flooding surface.

4.11. Facies 11: Limestone-marl alternation

Description

This heterolithic facies occurs above the Luxembourg sands and consists of a characteristic alternation of 10 to 20 cm thick limestone layers and interbedded marls (30 cm to 1 m in thickness). The limestones are composed of packestones with often large bivalve and ammonite fragments. The marls in between also have a very rich fauna consisting of gryphea, ammonites and crinoid particles.

Interpretation

The deposition of fine-grained marls and the increase in faunal activity implies deposition in a more open marine below wave base environment. In literature much debate arises whether these alternations are the result of climatologically variations with variable sediment input or just the end product of differential diagenesis (Westphal, 2006). Earlier studies on the Strassen Marls (Hanzo *et al*., 1994) concluded that there is some diagenetic control, but that based on palynology, the primary signal was likely to be climate controlled.

As the contribution focuses on the sandstone package, the diagenetic alterations in this limestone – marl sequence will not be further discussed. The interested reader is referred to the mentioned literature.

5. Detrital composition of the sandstones

Cemented and uncemented sands as well as coarse-grained bioclastic gravel lenses/layers display differences in detrital composition. This is due to a combination of differences in depositional environment, the intra- and extrabasinal derivation of sedimentary particles and post-depositional alteration of the detritals. The detrital composition varies between the different facies. Deeper facies are composed of silts and very fine-grained poorly sorted sands, whereas shallower facies consist of medium-grained, well-sorted sands. For carbonate rich samples (> 50 % carbonates) the Dunham (1962) classification scheme can be invoked.

Cemented sandstones can be classified as quartz arenites to calcarenites. They are dominated by subrounded mono- and polycrystalline quartz grains and variable amounts of carbonate grains including bioclasts, ooids and peloids. The ooids have a quartz or carbonate nucleus and a micritic or radiaxial fibrous cortex. Trace amounts (< 1%) of chert, lithic fragments (metasiltstones with rough cleavage; Garzanti & Vezzoli, 2003) and mica flakes (< 0.5%) are present as well as minor amounts of feldspar grains or their relict phases (5 to 10 %). Most of the feldspars have been dissolved or altered to kaolinite. Clays are concentrated as drapes or are infiltrated locally from overlying marls. They occur in trace (<1 %) to minor (only a few percentages) amounts in the fine-grained sediments. Within the different facies, trace to minor amounts of coal fragments are present along the stratification laminae. These are opaque and have polygonal cracks or exhibit cell textures. Most of the carbonate particles are micritised. Bioclasts show the development of a micritised rim or envelope (Pl. 1A-B). This micritisation results from borings by micro-organisms such as algae and bacteria (Smith & Nelson, 2003). Ooids with radiaxial cortex sometimes are completely micritised, with preservation of the original texture. The micrite envelope is covered by acicular cements. The former generally exhibits an orange luminescence colour, which is brighter than the acicular carbonate cements surrounding it. Deeper offshore facies (marls and very fine-grained sands) mainly consist of wackestones and packstones, carbonate rich samples in tidal influenced sandwaves are composed of packstones. The latter are dominated by peloids in a more distal environment and by ooids in a more proximal setting. Higher energy environments such as proximal sandwaves, sand dunes and birectional cross-stratified sandstones consist of grainstones.

The uncemented sands are mainly quartz arenites composed of mono- and polycrystalline quartz. Although small (up to 10%) amounts of carbonate particles, which mainly consist of stable crinoid particles, are locally present, the general absence of carbonate particles is the

main difference with the cemented rocks. Feldspars show lamellar dissolution and are altered to kaolinite. In fine-grained sands, more clays and coal fragments are present.

The coarse-grained bioclastic gravel bodies/layers show strong variation in detrital content ranging from siliciclastic to carbonate rich zones. Bioclastic rich layers contain up to 90% carbonate grains and are classified as rudstones. Carbonate content is determined by large bioclast shells (bivalves, ostracods and gastropods) and well developed ooids. Within the coarse-grained bioclastic gravel lenses/layers, three dominant types of pebble sized clasts are distinguished. Two groups of clasts are composed of calcite cemented sandstone. Type 1 comprises small (2 cm) well rounded pebbles and type 2 consists of well rounded, elongated or flat pebbles, up to 5 and 10 cm in length. Detrital composition of the cemented clasts generally is similar to the cemented sands. Type 1 clast is coarse-grained and moderately-sorted; type 2 clast is generally fine-grained and well-sorted. In some cases, type 2 clasts exhibit traces of small encrustations. Petrographically the two can be distinguished because of their different cement type as will be discussed below. The third group, extra-formational clasts, are well rounded and flattened quartzite and siltstone pebbles, generally 1 or 2 cm and sometimes up to 5 cm in size. The morphology and petrographic composition of these pebbles has been studied by Schreck (1976) and was used as provenance indicator.

6. Diagenetic phases

6.1. Carbonate phases

6.1.1. Calcite matrix

Based on their morphology, different types of diagenetic calcite can be differentiated within the lenses, i.e. acicular/columnar, syntaxial overgrowths, equant shaped calcites, sparitic and poikilotopic forms. The first calcite cement generation consists of acicular/columnar cement rims precipitated on carbonate particles. Around ooids and bioclasts generally well developed (50-100 µm) acicular crystals occur (Pl. 1A & 2A). In the fine-grained lithologies acicular cements are less common (Pl. 2B). The cements generally stain violet and exhibit a dull orange-red luminescence. The acicular cements present in the encrusted sandstone layer (= facies 10: hardground) on top of the sand succession stained red. The amount of acicular/columnar cement varies from 2 up to 10 % and in some cases it even completely fills intergranular primary pore space (~30 %).

Around echinoderms, a syntaxial overgrowth cement has formed (Pl. 1C-D), which exhibits red to violet staining colours and dull red luminescence. The size of these overgrowths varies from 10 up to 100 µm. Within cemented lenses they make up 5 to 10 %.

The remaining primary as well as secondary moldic porosity in the lenses has been filled by equant calcite cement (Pl. 1A-B). This cement can also be found as replacement of carbonate fragments. The size of the crystals is variable, ranging from a microsparite (30-50 µm) in the fine-grained sediments up to sparitic crystals (>100 µm) in larger primary and moldic pores. Crystal size increases towards the centre of a pore. Distinction between replaced grains and cemented moldic pores is made by equal crystal size or increasing crystal size respectively. With exception of few red staining samples taken from the fine-grained lithologies of Consdorf well cuttings, the equant cements stain violet-red to blue, which implies a ferroan nature. The cement is sometimes weakly sector zoned, displaying a dull red core and a more orange luminescent edge (Pl. 1E). Although the equant cements are related to the lenses, sometimes small patches of similar cements are present in the uncemented parts of the sandstone package. Quartz grains and their overgrowths (see below) are corroded by the equant cements which results in grains floating in the calcite matrix. Surface reaction and transport controlled corrosion textures are are recognised by oriented notches or regular shaped embayments with upstanding ridges (Pl. 2C) and irregular pits (Pl. 2E), respectively (Burley & Kantorowicz, 1986).

A fourth type of calcite cement consists of violet to blue stained sparitic to poikilotopic crystals. Poikilotopic crystals may have started to grow syntaxially around remaining echinoderms (Pl. 1F). Zones cemented by these calcites generally occur at the edges of the already formed lenses and within the cross-stratified sands as small concretions. These cements exhibit a dull red luminescence.

As mentioned in the paragraph on detrital composition, two types of calcite cemented reworked clasts are found

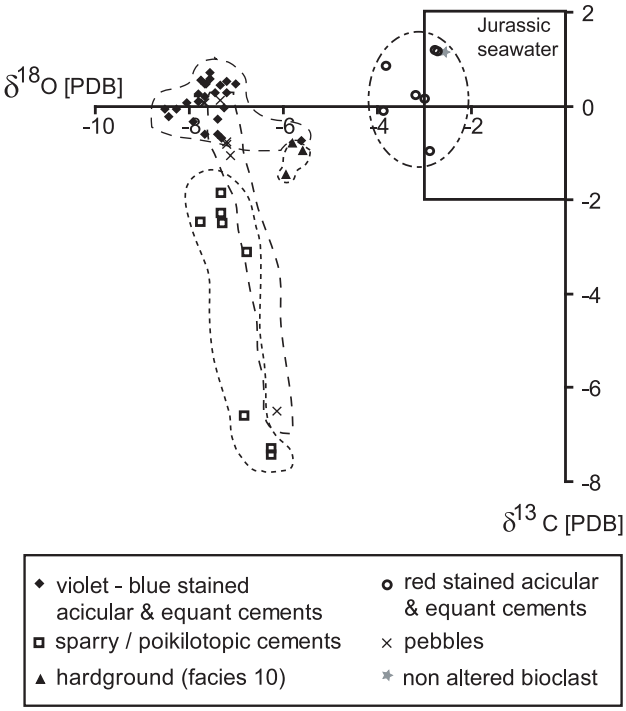

Figure 5. $\delta^{18}O$ - $\delta^{13}C$ cross plot of the different carbonate phases in the Luxembourg sandstone. Reference values for carbonates formed in equilibrium with Jurassic seawater were taken from literature (Jenkyns *et al.*, 2002).

in the coarse-grained gravel bodies and layers. These pebbles possess different types of calcite cement. Type 1 pebbles contain well developed red stained poikilotopic cements, which exhibit a strong alternation of bright and non luminescent zones (Pl. 1G). Although the poikilotopic nature of the cements is well developed, different pebble parts were replaced by a violet to blue stained equant cement with dull orange-red luminescence. Type 2 pebbles consist of blue stained acicular and equant cements. They display a dull orange-red luminescence similar as the equant cements in the lenses.

Several assumed non altered bioclasts were sampled and revealed a $\delta^{18}O$ value of approximately –2.7 ‰ and $\delta^{13}C$ value of +1 ‰ (Fig. 5). These values plot in the range of reference values for carbonates formed in equilibrium with Jurassic seawater (Jenkyns *et al.*, 2002). The acicular and equant cement types were bulk sampled for isotope analysis because of their small size. The samples with the red stained acicular and equant cements all have $\delta^{18}O$ values between -2 to -3 ‰. The $\delta^{18}O$ values from the violet blue stained equant cements all cluster at -8 to -7 ‰ and $\delta^{13}C$ values plot around 0 ‰ (Fig. 5). The values for the hardground on top of the Luxembourg Sandstone Formation (facies 10) show less negative $\delta^{18}O$ values than the other bulk sampled cements. The recrystallised bioclasts plot between -8 to -7 ‰ and $\delta^{13}C$ values plot around 0 ‰. The sparitic and poikilotopic cements show a trend towards slightly more negative $\delta^{13}C$ values (up to -8 ‰), while they have the same $\delta^{18}O$ values as the equant cements.

The two clasts can also geochemically be differentiated. The type 1 clasts plot along a trend line between –7 and 0 for $\delta^{13}C$ with $\delta^{18}O$ values ranging between -6 and -8. The trend line, having an intercept with the $\delta^{13}C$ axis at -12, is however less steep than that of the poikilotopic/sparitic cements with an intercept at -19. The mixing trend is a result of the earlier described replacement of the poikilotopic by equant cements. The type two clasts integrally plot within the same range as the violet-blue stained cements. Their $\delta^{18}O$ values mainly range between -7 and -8, the $\delta^{13}C$ values between -1 and 1. This confirms the theory that type 2 clasts are intraformational reworked. No similar in situ cemented horizons were observed for type 1 clasts. This means that there is no clear evidence whether they are intra- or extraformational.

6.1.2. Veins

Two vein types, a thick (> 2mm) and thin (< 2mm) vein, cut across the cemented lenses. The thick vein type is composed of two calcite cement generations. The first cement generation along the edge of the thicker veins is characterised by violet stained sparitic and radiaxial calcite cements with dull luminescence. They do not show zonation and have a dusty appearance due to the high amount of inclusions (organic matter, clay, fluid). The second cement generation in the thicker vein type is a blue to red stained, sparitic calcite cement with zoned dull red to orange luminescence. The latter cement generation also fills the thin veins. The isotope signature of the vein cements (for clarity no shown) plot in a similar range as the violet blue stained equant cements with $\delta^{18}O$ ranging from -6 to -8 and $\delta^{13}C$ from -1 to 1.

6.1.3. Dolomite

Dolomite crystals were observed in very small trace-amounts as micro-rhombohedral inclusions in between calcite cements. Additionally, their former presence is suggested by the outline of dissolved rhombohedra marked by iron oxide rims.

6.2. Non-carbonate phases

6.2.1. Pyrite

Small amounts of pyrite (< 1%) generally occur within the fine-grained sediments. Although often masked by a rim of iron oxides, pyrite occurs as small framboids (10-50 μm) or may display more euhedral forms (10 μm in size). They are disseminated throughout the sediment within inter- and intragranular pores, related to clay drapes (Pl. 2D) and coal fragments or in the vicinity of bioclasts fragments. Pyrite formed more abundantly within the hardground at the contact between the Luxembourg sands and the Strassen Marls.

6.2.2. Quartz overgrowths

Euhedral quartz cements (< 3%) are present in the zones without important calcite cements (Pl. 2E). Some syntaxial overgrowths were recognised around monocrystalline quartz grains. The presence of clay rims on the quartz grains generally results in the formation of irregular overgrowths. Quartz overgrowths are sometimes strongly corroded by the equant calcite cements, which implies they predate this cement generation.

6.2.3. Kaolinite

Kaolinite is found in minor amounts (up to 5%) in primary pores of uncemented sandstone (Pl. 2E) and secondary pores of both cemented and uncemented sandstones. Association with altered feldspars or secondary pores and well developed booklet structures (Pl. 2F) indicates it formed by alteration of feldspars.

6.2.4. Iron oxides

In the uncemented sands, iron oxide precipitates are present as coatings on quartz grains and they mark the presence of dissolved particles and cements. Within the cemented lenses, these oxides can be found within secondary pores. It is likely that iron oxides have formed as a sub-recent alteration product when oxygen rich waters infiltrated the sandstones and altered the dispersed pyrite.

6.3 Compaction and porosity evolution

Evidence for mechanical compaction is restricted to minor deformation of ductile grains such as muscovite (Pl. 1H) and peloids. The presence of clay drapes over the equant cements along the edges of the cemented lenses suggests that sufficient burial took place after this cementation period (Pl. 2D). The maximum burial depth of the

Facies	height (see Fig 3)	Cementation	Qtz (M&P)	Fsp	Ooid/ peloid	Bioclast	Ech.	replaced	SP	micrite	acicular cement	syntaxial cement	equant cement	sparry/poik. cement	quartz cement	Kaolinite	opake phase	Fe-oxides	PP	other	IGV
1		uncemented	65,2	2,0	0,0	0,2	0,0	0,0	4,2	0,0	0,0	0,0	0,0	0,0	1,4	0,6	0,0	5,2	21,2	0,0	28,4
1		uncemented	74,4	1,2	0,0	0,0	0,0	0,0	0,6	0,0	0,0	0,0	0,2	0,0	0,8	0,8	0,0	2,2	19,8	0,0	24,4
2	8,90 m	cemented layer	28,6	2,9	9,9	5,2	0,0	0,0	0,4	0,0	2,6	0,0	49,7	0,0	0,7	0,0	0,0	0,1	0,0	0,0	52,9
2	8,90 m	cemented layer	29,3	0,7	1,0	0,2	3,4	3,3	1,4	5,6	0,1	0,8	47,2	2,5	0,0	0,4	1,5	2,6	0,0	0,0	50,6
3	9,90 m	cemented layer	21,3	0,4	7,2	0,5	5,7	2,0	1,1	0,7	0,5	0,7	56,8	2,4	0,0	0,1	0,3	0,2	0,0	0,1	60,4
3	9,20 m	cemented layer	33,6	1,8	2,4	0,0	4,5	0,8	1,4	7,1	0,0	2,0	27,0	6,6	0,0	0,3	5,8	0,5	6,3	0,1	41,9
4 tot 6	12,90 m	cemented lens	28,2	3,7	15,6	2,3	0,0	0,0	7,1	0,0	9,8	0,0	32,8	0,0	1,4	0,0	0,0	0,1	0,0	0,0	44,0
4 tot 6	13,50 m	uncemented & small concretion	53,7	2,6	0,0	0,1	0,7	0,8	3,1	0,8	0,0	1,7	7,3	10,6	1,0	1,2	0,2	6,2	9,7	0,1	30,5
4 tot 6	15,00 m	cemented lens	35,4	2,8	3,0	0,6	3,4	7,6	6,8	2,9	0,9	6,6	26,4	1,2	0,2	0,5	0,0	1,0	0,3	0,4	35,6
4 tot 6	16,00 m	cemented lens centre	40,3	2,5	3,5	0,1	2,3	6,6	5,9	3,3	4,3	2,4	26,9	0,4	0,8	0,3	0,0	0,5	0,3	0,0	34,9
4 tot 6	16,00 m	cemented lens edge	57,1	2,1	0,1	0,3	0,6	0,1	0,4	1,3	0,0	2,7	22,7	1,8	1,1	0,3	0,0	2,2	7,1	0,0	35,3
4 tot 6	16,20 m	cemented lens centre	33,0	1,4	4,6	0,1	1,5	5,8	8,7	4,5	5,6	3,8	27,9	0,4	0,1	0,5	0,8	0,7	0,5	0,1	38,3
4 tot 6	16,20 m	cemented lens edge	42,3	1,3	0,0	0,0	2,3	5,3	1,7	2,7	0,0	10,0	28,3	4,7	0,7	0,0	0,0	0,7	0,0	0,0	34,2
4 tot 6	16,20 m	uncemented sand	51,7	1,3	0,5	0,0	3,7	0,5	4,5	0,0	0,0	3,8	5,3	1,3	0,0	0,3	0,0	3,3	23,7	0,0	43,7
4 tot 6	16,30 m	cemented lens	54,1	1,4	0,2	0,2	4,1	4,4	2,5	3,2	0,0	4,1	21,6	1,3	0,2	0,2	0,4	0,8	1,3	0,0	28,5
4 tot 6	17,00 m	cemented lens	42,8	0,6	3,1	0,1	4,2	6,0	6,8	4,4	0,8	6,9	21,3	1,4	0,2	0,1	0,0	0,4	0,9	0,0	31,5
4 tot 6	23,00 m	uncemented sands	53,2	3,8	0,0	0,0	0,0	0,0	3,2	0,0	0,0	0,0	1,2	0,0	2,2	0,6	0,0	6,6	29,2	0,0	32,6
8	34,00 m	cemented stormlayer	5,3	0,5	0,4	2,9	6,4	13,3	11,7	1,4	7,7	9,3	39,7	0,0	0,0	0,1	0,0	0,6	0,7	0,0	57,4
8	34,00 m	cemented channel top	33,4	0,9	3,5	0,4	0,9	6,9	6,5	1,4	7,2	1,8	23,8	10,3	0,1	0,3	0,7	1,6	0,0	0,0	43,2
8	34,00 m	cemented channel base	16,6	0,0	0,2	8,0	1,6	10,4	3,8	1,4	3,8	0,8	0,8	32,0	0,0	1,0	0,2	1,0	1,2	0,0	38,6
9		cemented channels	19,5	5,1	11,0	6,8	0,0	0,0	2,1	0,0	6,3	0,0	46,4	0,0	0,8	0,0	0,0	2,1	0,0	0,0	53,4
9			40,8	3,9	4,6	2,7	0,0	0,0	8,0	0,0	1,0	0,0	32,9	0,0	2,9	0,0	0,0	0,2	3,1	0,0	39,9
9			30,9	5,2	9,4	5,4	0,0	0,0	7,0	0,0	6,7	0,0	34,6	0,0	0,2	0,0	0,0	0,3	0,2	0,0	41,7
9			31,2	1,8	0,8	0,0	2,6	7,0	7,1	1,5	4,4	2,5	35,1	4,7	0,0	0,6	0,0	0,7	0,0	0,0	46,7
9			40,2	3,7	7,4	5,3	0,0	0,0	4,0	0,0	3,6	0,0	32,8	0,0	0,3	0,0	0,0	2,6	0,1	0,0	36,8
9			56,1	4,2	0,3	0,1	0,0	0,0	4,1	0,0	0,0	0,0	7,7	0,0	2,7	0,0	0,0	2,4	21,8	0,0	32,1
9			30,3	1,9	4,1	8,9	0,0	0,0	11,0	0,0	4,6	0,0	36,9	0,0	0,4	0,0	0,0	0,4	1,4	0,0	43,3
10	50,00 m	harground top	21,3	1,5	11,2	0,1	0,6	3,3	1,1	1,3	6,9	0,1	3,9	9,6	0,0	0,0	37,0	2,1	0,0	0,0	20,5
8 and 9		type 1 clast (*)	58,0	0,0	2,5	1,2	0,0	0,0	1,2	0,0	0,0	0,0	0,0	37,0(**)	0,0	0,0	0,0	0,0	0,0	0,0	37,0
8 and 9		type 2 clast (*)	31,2	0,0	12,9	1,1	0,0	0,0	21,5	0,0	3,2	0,0	30,1	0,0	0,0	0,0	0,0	0,0	0,0	0,0	33,3

Table 2: Point counting data (1000 points counted) from the different sections. Qtz: quartz (M: monocrystalline; P: polycrystalline); Fsp: feldspar; Ech.: echinoderm fragments; replaced: replaced ooids/bioclasts; SP: secondary porosity; poik: poikilotopic; PP: primary porosity; IGV: Intergranular Volume. The internal composition of the clasts was determined during the counting and recalculated to 100 %. The poikilotopic cement in type 1 clast (**) is a different cement type (bright-non zoned), than the poikilotopic cements in the cemented zones.

sandstone formation was approximately 500 m (Berners, 1985). At certain levels in the uncemented parts, quartz grains have suffered some chemical compaction leading to planar and slightly curved contacts. The high minus cement porosity (with values up to 50 %) of the cemented layers (Tab. 2), clearly suggests that calcite cementation started early and stabilised the framework. Based on the minus cement porosity, a difference in degree of compaction of 10% between the cemented and uncemented layers is deduced (Tab. 2).

All primary porosity in the cemented lenses and layers has been reduced to zero. Moldic porosity was created by dissolution of unstable particles such as shell fragments or ooid cortices and feldspars. The secondary pores left behind, are partially to completely refilled by spar-sized equant calcite cements and kaolinite respectively.

In the uncemented layers primary porosity has been preserved and additionally secondary porosity is marked by oversized pores. Based on corrosion textures of quartz grains, it can be assumed that some cement which was present in the present-day uncemented layers has been dissolved.

Telogenetic alterations resulted in additional creation of secondary molds by dissolution of (unstable) carbonate particles and cement dissolution. Especially cemented layers in outcrops have higher moldic porosity.

6.4 Modal composition

Based on the point counting results (Tab. 2), the original detrital composition of the deposited sands is calculated and plotted (Fig. 6) in a three component system with quartz, feldspar and carbonate particles as end members. Therefore, the secondary porosity is interpreted to be the result of dissolution either of carbonate particles or feldspars depending on the shape of the mold or oversized pore, the presence of kaolinite or calcite cement in the mold and occurrence in cemented or uncemented layer. Replaced and refilled carbonate fragments were counted as a separate phase in order to get information on the original detrital composition and amount of replacement. These criteria were used to recalculate the detrital composition after deposition of the sands and therefore some minor discrepancies might exist which are in the order of several percentages. The relationship between detrital composition and diagenesis is shown by plotting the data as a function of the amount of carbonate cement (Fig. 6) counted in the thin sections. Based on the triangle plot the relationship between the amount of calcite cement and the sedimentary composition is clearly revealed. More carbonate cement is found in zones with high detrital carbonate content.

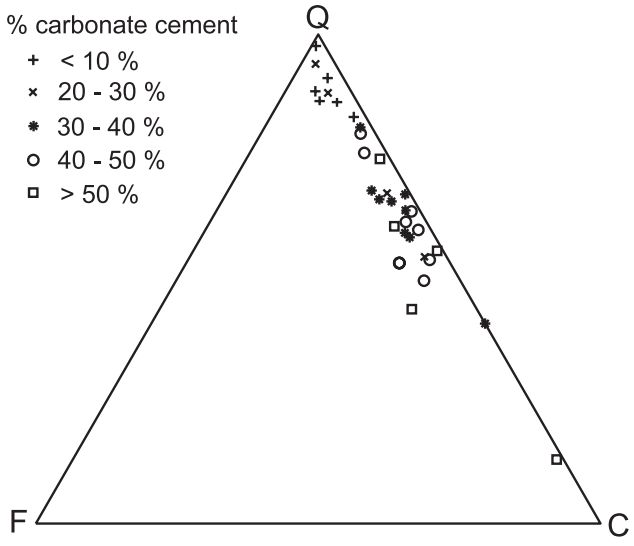

Figure 6. Plot of the restored modal composition (see text) of the deposited sands. Three component system plot with quartz (Q), feldspar (F) and carbonate (C) particles. Used symbols refer to the amount of carbonate cement present in the sandstones.

7. Discussion

The paragenesis of the Luxembourg Sandstone Formation is shown in Fig. 7. The cement morphology (Harris *et al.*, 1985), the high intergranular volume of the cemented lenses (Tab. 2) and the presence of large reworked calcite cemented pebbles containing sometimes small encrustations/bioturbations all give evidence that cementation started at or close to the seawater-sediment contact.

Two types of calcite cemented reworked clasts were distinguished. The presence of both acicular and equant cements in type 2 clast, suggest that these two cement types formed before reworking (Wilkinson *et al.*, 1985; Molenaar, 1990). The origin of the type 1 cemented clast is less clear, because no cemented horizons with the same characteristics were found in situ. Based on the sedimentary composition, however, one can assume they also are intraformational reworked and possibly were formed at very shallow water depths in oxic to suboxic conditions and in presence of organic matter and meteoric waters, as shown by their variable cathodoluminescence and oxygen isotopic composition of -6 to -8 ‰.

Precipitation of acicular calcite cements was preceded by micritisation of carbonate fragments and probably occurred in the oxic zone, close to the seawater-sediment interface. In the bacterial sulphate reduction zone pyrite was formed as a result of bacterial degradation of organic matter. This is indicated by the framboids, the relationship with organic and fine grained matter or bioclast fragments. Oxidised organic carbon however did not contributed to the source bicarbonate for cementation.

Upon burial, the equant calcite cements not only cemented primary pore space, but also characterise replaced shell fragments. Neomorphism generally occurs when a less stable aragonite or high magnesium calcite precursor is replaced by a more stable calcite (Hendry *et al.*, 1995; Maliva *et al.*, 2000). The excess Mg will precipitate as small dolomite phases.

The poikilotopic and sparitic calcite cements which occur at the outer sides of the cemented lenses and within smaller nodules in the uncemented sands, are interpreted as diagenetic precipitates which formed after burial and in relation to the influx of meteoric water. The small nodular forms in the uncemented sands can be linked to the presence of echinoderm fragments where late diagenetic syntaxial cements precipitated and further grew out as poikilotopic and sparitic cements. The late diagenetic origin of these cements is supported by the lower (e.g. 34 % at the edge vs. 38 % in the centre) intergranular volume (Tab. 2), if compared to the intergranular volume registered in the nearby cemented lenses.

The different early diagenetic processes can be

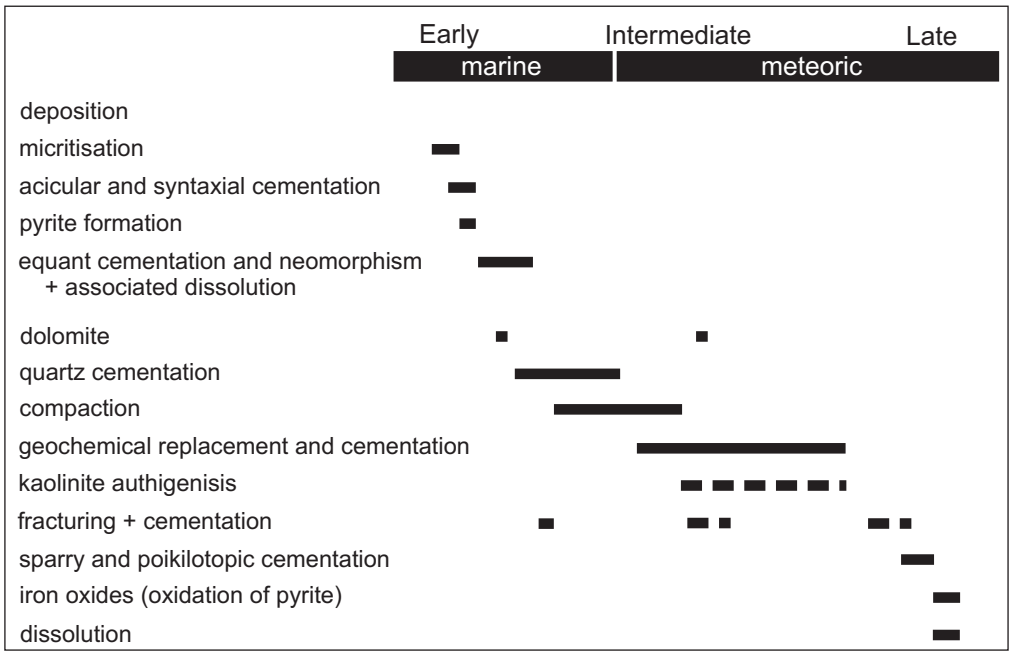

Figure 7. Paragenetic sequence of the Luxembourg Sandstone Formation. Discussion of the main steps in the text.

grouped in either advection controlled or diffusion controlled processes (Berner, 1980). Walderhaug and Bjørkum (1998) further suggested that the nucleation site distribution can be used to figure out whether a cementation process was more advection or diffusion controlled. In the early diagenetically cemented lenses of the Luxembourg sands, the distribution of the carbonate fragments which acted as nucleation sites for the first cement generation are located close to each other which implies that cementation likely was controlled by advection. A possible source and process to initiate cementation is the flow of saturated seawater through the sediment, as suggested by Molenaar (1998). A possible mechanism for pore water flow is related to tidal pumping and wave activity. Besides a high degree of $CaCO^3$ (super)saturation and presence of a suitable stable substrate, also high rates of water exchange within the substrate and time will be important parameters to fulfil (Nelson & James, 2000). With respect to water exchange, this implies that permeability is an important parameter for this first cement generation. Marshall and Ashton (1980) provided evidence from Jurassic hardgrounds of the Lincolnshire Limestone Formation that the higher permeability systems favour growth of longer crystals. This relationship might hold also for the acicular cements in the Luxembourg Sandstone Formation. The depth to which tidal pumping affected the Luxembourg sands is not clear. The sedimentary architecture however provides evidence that this depth likely was limited because the presence of sedimentary permeability barriers, such as clay drapes along the reactivation surfaces as well as by cementation.

The red stained equant calcite cement generation also points to a marine origin as supported by the isotope values obtained from the Consdorf well cuttings (Fig. 5). The source of this calcite cement might come from redistribution of carbonate fragments from the intervals, which were not affected by the first cement generation. This is evidenced by the fact that on a very small lateral and vertical scale there is a sharp transition between cemented sediment containing a high amount of carbonate fragments (bivalve shells, ooids) and sediment without carbonate fragments. Only echinoderm fragments have survived dissolution in the uncemented layers, because they generally are more stable (Smith & Nelson, 2003). Recently, James *et al*. (2005) demonstrated that during shallow marine burial up to 80 % of the skeletal aragonite can be lost due to dissolution in seawater. They suggested that based on some recent studies, aragonite can be dissolved as a by-product of bacterial degradation of organic matter. If this is the case, the uncemented layers possibly contained originally more carbonate fragments after deposition than one can observe today. Bivalve shells and ooid cortices have dissolved and caused cementation. Due to ongoing compaction remaining porosity gradually decreased. The influence of bacterial biodegradation is evidenced by the presence of pyrite framboids which occur dispersed in the sediment. It should be noted that biodegradation can not be invoked as a HCO^3- source for cementation since $\delta^{13}C$ shows no depletion.

After burial, influx of unsaturated meteoric waters changed the geochemical signature of the carbonate cements. This is shown by the shift to more depleted $\delta^{18}O$ values and blue stain for the equant and acicular cements (compare with Wilkinson, 1993). Additional cementation on remaining echinoderm fragments resulted in the formation of small nodular calcite cemented geometries and zones of sparitic to poikilotopic cements along the edge of the lenses. Unstable skeletal fragments which survived earlier dissolution likely were the source of the calcite. The $\delta^{13}C$ values show that minor soil gas was involved (Muchez *et al*., 1993). The nodular cemented geometries are typically aligned along the stratification laminae, which relates to the distribution of the echinoderm fragments along the foreset laminae. It is along the latter that the paleo-groundwater flow direction preferentially occurred and gave rise to nodule formation (McBride *et al*., 1994; Mozley & Davis, 1996).

The $\delta^{18}O$ isotope signatures of the veins (between -7 and -8) indicate they have formed in a meteoric environment. The staining characteristics the thick veins, shows an increase in Fe towards the centre. The inclusion rich zone and dusty luminescence characteristics along the edges of the thicker veins indicate that they have been recrystallised. The sometimes radiaxial outline of this cement generation supports a Mg rich precursor and thus an original acicular outline, which likely formed in marine pore waters (Wilson & Dickson, 1996). Similar textures are described by Marshall (1981) in ammonite chambers from the Jurassic Bearreraig Sandstone Formation.

The second calcite cement generation formed in optical continuity with the first cement generation and formed in the meteoric environment. This fracturing is thus related to relative uplift and influx of meteoric waters. The fracturing probably reactivated the thicker veins and created new thinner veins. The 13C values indicate that carbonate was sourced by internal redistribution.

8. Facies and cementation patterns

From the previous discussion it is clear that the geometry and distribution of carbonate cemented zones can be related to the first cement generation which was subsequently enhanced by redistribution of carbonate from the uncemented into the cemented layers. To start cementation, in general several conditions have to be fulfilled, namely: existence of a calcite providing a saturated fluid (seawater) and the presence of carbonate catalysing nucleating sites. Two additional parameters will have control on cement distribution and resulting geometry of cemented zones: (1) permeability variations to create localised fluid flow; (2) residence time within influence of calcite saturated water, in this case seawater. It is clear that for the first cement generation, these parameters are strongly related to the depositional environment and thus a linkage can be made between this type of cementation and the depositional setting, i.e. facies. The influence of these parameters will be discussed below and in Fig. 8 a schematic relationship between the

sandstone architecture and cementation is shown. The following remarks can be made:

8.1. Diagenesis of homogeneous sands and storm sand beds (Facies 1 and 7)

As mentioned above, this facies generally occurs at the base of the Luxembourg sands. Its deposition is prior to the development of the prograding sandbar system and not represented in the sketch of Fig. 8. The absence of any major cementation likely relates to the original detrital content which was dominantly terrigeneous. This detrital mineralogy is related to the transgressive system and absence of a carbonate generation bio-system. In addition, the homogeneous nature of these sediments will favour a more homogeneous diffuse fluid flow, and thus localised fluid flow does not occur. As these sediments are interpreted to result from fast deposition, residence time near the seawater contact was too limited to provoke precipitation of the first cement generation. The absence of calcite cements in the storm deposited sand beds might be related to the rapid burial of these sands.

8.2. Diagenesis of the marls and very fine-grained sands (Facies 2 and 3)

In the marls, cementation occurs in coarser-grained horizontal limestone beds (Fig. 8), which were interpreted to be related to storm events. The high amount of bioclast fragments in these layers are ideal nucleation sites and the grain size is sufficiently higher than in the underlying marls and very fine-grained sands, which results in good permeability contrast. Cementation thus could start along the entire layer. The flux of seawater through the sediment

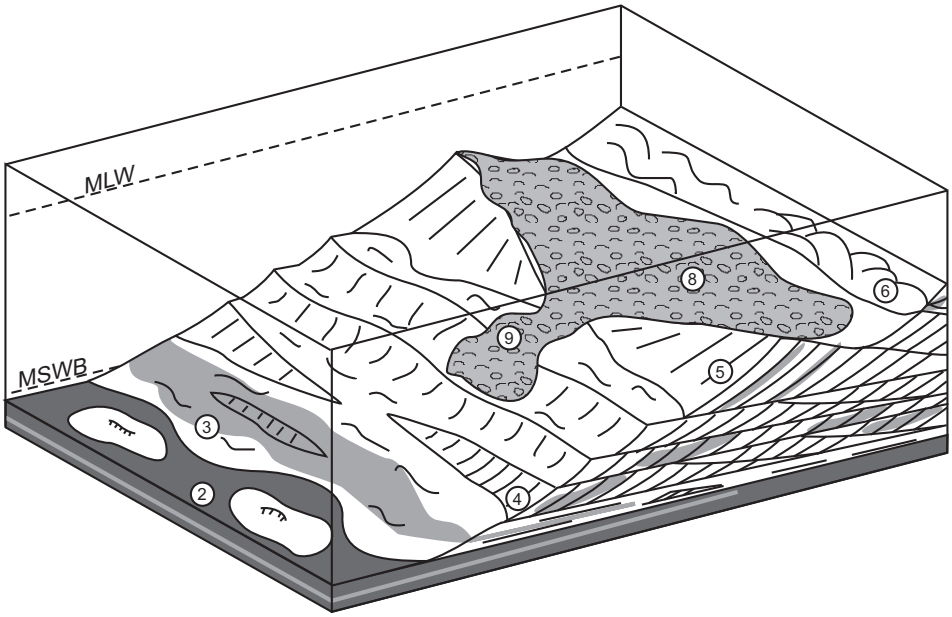

Marls and very fine grained sands

Cementation in:
- Coarser bioclastic rich storm layers
- Lensoid in most permeable zone of cross stratified sandsheets
- Top of sandsheets or coarse grained zones in the marls
- Related to prolonged residence time

Cross-stratified sandstone layers

Cementation as lenses and semi-continuous layers
- Well sorted sands
- Carbonate rich zones
- Permeability variation caused by grain size variability resulting from variable hydrodynamic conditions in a tidal influenced environment
- Residence time strongly determined by migration pattern of the sandwaves

Coarse grained gravel layers and channels

Continuous cementation and as lenses (channel outline) respectively
- Accumulation of coarse grained material: extra- and intraformational pebbles, bioclasts
- Higher permeability than surrounding strata which results in longer period of seawater flow

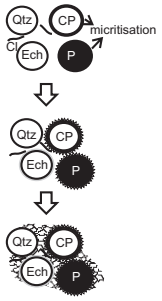

CP: small bioclast fragments
P: Peloids
Ech: Echinoderms
Cl: clays
Qtz: Quartz

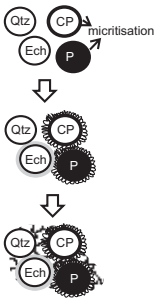

CP: ooids, bioclast fragments
P: peloids

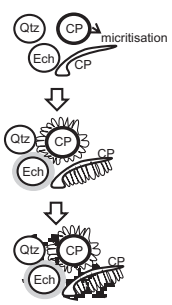

CP: ooids, bioclast fragments, bivalve fragments

+ Hardground on top

Continuous cemented flooding surface
- High amount of carbonate fragments
- Prolonged exposure time during sea level rise

Figure 8. Schematic representation of a prograding sequence showing the distribution and geometry of carbonate cemented zones and depositional architecture (not to scale). Numbers refer to different facies. Storm facies, hardground on top and overlying marls are omitted from the sketch. Qtz: Quartz particles; CP: carbonate particles (specified for different facies and additional P: peloids); Ech: Echinoderm fragments; Cl: clays.

decreased and cementation likely continued by diffusion (e.g. Ketzer *et al.*, 2002), when overlying marls were deposited.

In the very fine-grained sands, cementation gives rise to as horizontal layers and lenses. Carbonate particles such as peloids and small bioclasts fragments in the cemented zones are well preserved. There are different amounts of clay in the uncemented and cemented layers. The higher amount of clays in the now uncemented layers originally resulted in lower permeability. Cementation likely was predominant during periods of non deposition at the seawater-sediment contact. Fluid flow was however limited and only small acicular cement fringes developed.

8.3. Diagenesis of the cross-stratified sandstones (Facies 4, 5 and 6)

In the fine to medium-grained sands, acicular cements on carbonate particles and syntaxial overgrowths on echinoderms are well developed (Fig. 8). Point counting analyses show these cements are volumetrically more abundant than in the very fine-grained cemented layers. Cementation started in the centre of the cross-stratified lenses with highest amount of carbonate fragments and most likely in the most permeable zones. Variation in flow velocity during deposition of the sands results in subtle grain size variations as well as small compositional variations (Hartkamp *et al.*, 1993). This variability even can be seen on thin section scale (Figs 4D; Pl. 1C-D). Obviously, during bedform migration, deposition of coarser material is related to high flow velocities, which can in tidal influenced environments be related to the so called hydrodynamic full-vortex stage of bedform migration in a spring cycle (Boersma & Terwindt, 1981). Clay drapes along the foresets were deposited during slackening periods. The sedimentary structures mostly are bounded at the base by reactivation surfaces, sometimes also marked by fine clay drapes. Bottom and top sets are often slightly bioturbated. The latter features resulted in thin zones with generally lower permeability.

As the duration of exposure to seawater pore-circulation is also an important factor, only beds which have remained in direct contact to seawater for a longer period became cemented. If a cross-stratified layer became rapidly buried by migration of prograding and aggrading sediments, the likeliness that cementation took place in the older layer decreased.

8.4. Diagenesis of coarse-grained channels and gravel layers (Facies 8 & 9)

The channels and gravel layers are very coarse in contrast with the generally fine to medium-grained surrounding sands. Although the gravel layers are less well-sorted, the effective porosity was high due to the framework nature of the bioclasts and thus permeability was higher than in the surrounding sands. Therefore preferential fluid flow will take place in these coarse-grained bioclastic gravel layers. In addition, the accumulated bioclasts provided a high amount of nucleation sites to initiate cementation.

8.5. Diagenesis at the contact with overlying marls unit (Marls of Strassen, Facies 10)

The top of the Luxembourg Sandstones is marked by the development of a hardground above which more open marine conditions were installed, as shown by the marls and faunal activity (gryphea and crinoids). The sands of this hardground are well-sorted and composed of a high amount of carbonate fragments. Development of this cemented layer fits the general concept that deepening of the basin, resulted in a more prolonged residence time of the flooding surface at the seawater contact with the laterally extensive development of carbonate cementation (Al-Ramadam *et al.*, 2005; Machent *et al.*, 2007). The interaction with the seawater decreased when overlying marls were deposited. The latter also created anoxic conditions which favoured bacterial sulphate reduction explaining the higher amount of pyrite at this contact.

9. Conclusions

Sedimentary architecture exerts a major control on calcite cementation in the Luxembourg Sandstone in many aspects. The direct impact of these parameters is shown by the distribution of the first acicular/columnar and syntaxial cement generation:

Sedimentary architecture determines the geometry of cemented zones. Depositional fabric is strongly related to the hydrodynamics of the basin and the sedimentary structures will determine porosity/permeability distributions, favouring fluid flow for later cementation.

Sedimentary composition, i.e. presence of carbonate grains in the Luxembourg sands, determines the presence of nucleation sites. It should be noted that a strong relation exists between the hydrodynamics and the sedimentary composition, as evidenced by accumulation of carbonate fragments in lag deposits and channel fills, which gernerate continuous cemented layers and well developed cemented bodies respectively.

Prolonged residence time at or close to the seawater contact additionally favours cementation. This parameter determines the ability of the sediment to stay within the influence zone of saturated flushing seawater. This is especially shown in the cross-stratified sandstone layers with different cemented lenses and the hardground on top of the formation, which is continuously cemented. The latter also gives direct evidence of this prolonged residence time.

The sedimentary composition will also influence later cement generations. Detrital carbonate will act as source for equant calcite cement and sparitic calcite cement during internal carbonate redistribution from the uncemented layers into the early cemented zones. This takes places during marine burial and even later in the meteoric realm. In addition, remaining echinoderm fragments in uncemented layers provided nucleation sites for later small scale nodular calcite cemented zones.

10. Acknowledgements

The authors like to thank the Feidt Company in Luxembourg for the visits to the quarries. P. Wertz (Feidt Company) is thanked for his assistance and useful comments during fieldwork. R. Maquil and R. Colbach (Geological Survey of Luxembourg) provided the well cuttings. The fruitful discussions with Prof. Dr. N. Vandenberghe and Prof. Dr. Ph. Muchez (Geology Section, K. U. Leuven) greatly improved the interpretations in this work. Prof. F. Boulvain (Geology Department, Université de Liège) and an anonymous reviewer are thanked for useful comments. Thin sections have been kindly prepared by H. Nijs (Geology section, K. U. Leuven) and D. Steeno (Geology section, K. U. Leuven) transferred the idea of developing an excel controlled point counting device into reality. Stable isotope analyses were carried out by Prof. Dr. M. Joachimski (University of Erlangen, Germany).

References

AIGNER, T., 1985. *Storm Depositional Systems: Dynamic Stratigraphy in Modern and Ancient Shallow-Marine Sequences*. Lecture Notes in Earth Sciences, 3. Springer-Verlag, Berlin, 174 pp.

ALLEN, J.R.L., 1963. The classification of cross-stratified units. With notes on their origin. *Sedimentology*, 2: 93-114.

ALLEN, J.R.L., 1980. Sand Waves - a Model of Origin and Internal Structure. *Sedimentary Geology*, 26: 281-328.

ALLEN, J.R.L. 1984. *Sedimentary Structures: Their Character and Physical Basis*. Developments in Sedimentology, 30 A+B. Elsevier, Amsterdam, 663 pp.

AL-RAMADAN, K., MORAD, S., PROUST, J.N. & AL-AASM, I., 2005. Distribution of diagenetic alterations in siliciclastic shoreface deposits within a sequence stratigraphic framework: Evidence from the Upper Jurassic, Boulonnais, NW France. *Journal of Sedimentary Research*, 75: 943-959.

ANDERTON, R. 1976. Tidal-Shelf Sedimentation - Example from Scottish Dalradian. *Sedimentology*, 23: 429-458.

BERNER, R.A., 1980. *Early Diagenesis: A Theoretical Approach*. Princeton Series in Geochemistry. Princeton University Press, Princeton, 241 pp.

BERNERS, H.P., 1983. A lower Liassic offshore bar environment, contribution to the sedimentology of the Luxemburg Sandstone. *Annales de la Société Géologique de Belgique,* 106: 87-102.

BERNERS, H.P., 1985. *Der Einfluss der Siercker Schwelle auf die Faziesverteilungen meso-känozoischer Sedimente im NE des Pariser Beckens: Ein Sedimentationsmodell zum Luxemburger Sandstein (Lias), spezielle Aspekte zur structurellen Änderung der Beckenconfiguration und zum naturräumlichen Potential*. PhD dissertation, Rheinisch-Westfälischen Technische Hochschule, Aachen, Germany, 321 pp.

BJØRKLYKKE, K. & BRENSDAL, A., 1986. Diagenesis of the Brent Sandstone in the Statfjord field, North Sea. *In* Gautiers, D.L., (ed.), *Roles of organic matter in sediment diagenesis*, SEPM Special Publication, 38. The Society of Economic Paleontologists and Mineralogists, Tulsa, 157-167.

BJØRKUM, P.A. & WALDERHAUG, O., 1993. Isotopic Composition of a Calcite-Cemented Layer in the Lower Jurassic Bridport Sands, Southern England - Implications for Formation of Laterally Extensive Calcite-Cemented Layers. *Journal of Sedimentary Petrology,* 63: 678-682.

BLOTT, S.J. & PYE, K., 2001. GRADISTAT: A grain size distribution and statistics package for the analysis of unconsolidated sediments. *Earth Surface Processes and Landforms*, 26: 1237-1248.

BOERSMA, J.R. & TERWINDT, J.H.J., 1981. Neap-Spring Tide Sequences of Inter-Tidal Shoal Deposits in a Mesotidal Estuary. *Sedimentology*, 28: 151-170.

BOULVAIN, F., BELANGER, I., DELSATE, D., DOSQUET, D., GHYSEL, P., GODEFROIT, P., LALOUX, M., ROCHE, M., TEERLINCK, H. & THOREZ, J., 2000. New lithostratigraphical, sedimentological, mineralogical and paleontological data on the Mesozoic of Belgian Lorraine: a progress report. *Geologica Belgica*, 3: 1-33.

BOULVAIN, F., BELANGER, I., DELSATE, D., GHYSEL, P., GODEFROIT, P., LALOUX, M., MONTEYNE, R. & ROCHE, M., 2001. Triassic and jurassic lithostratigraphic units (Belgian Lorraine). Geologica Belgica, 4: 113-119.

BOURQUIN, S., PERON, S. & DURAND, M. 2006. Lower Triassic sequence stratigraphy of the western part of the Germanic Basin (west of Black Forest): Fluvial system evolution through time and space. *Sedimentary Geology*, 186: 187-211.

BURLEY, S.D. & KANTOROWICZ, J.D., 1986. Thin-Section and Sem Textural Criteria for the Recognition of Cement-Dissolution Porosity in Sandstones. *Sedimentology*, 33: 587-604.

BURNS, F.E., BURLEY, S.D., GAWTHORPE, R.L. & POLLARD, J.E., 2005. Diagenetic signatures of stratal surfaces in the Upper Jurassic Fulmar Formation, Central North Sea, UKCS. *Sedimentology*, 52: 1155-1185.

DE GRACIANSKY, P.-C., JACQUIN, T. & HESSELBO, S.P. 1998a. The Ligurian cycle: an overview of lower jurassic 2nd order transgressive/regressive facies cycles in Western Europe. *In* De Graciansky, P.-C., Hardenbol, J., Jacquin, T. and Vail, P.R., (eds), *Mesozoic and Cenozoic sequence stratigraphy of European basins*, SEPM Special Publication, 60. The Society of Economic Paleontologists and Mineralogists, Tulsa, 467-479.

DE GRACIANSKY, P.-C., DARDEAU, G., DOMMERGUES, J.L., DURLET, C., MARCHAND, D., DUMONT, T., HESSELBO, S.P., JACQUIN, T., GOGGIN, V., MEISTER, C., MOUTERDE, R., REY, J. & VAIL, P.R., 1998b. Ammonite biostratigraphic correlation and Early Jurassic sequence stratigraphy in France: comparison with some U.K. sections. *In* De Graciansky, P.-C., Hardenbol, J., Jacquin, T. and Vail, P.R., (eds), *Mesozoic and Cenozoic sequence stratigraphy of European basins,* SEPM Special Publication, 60. The Society of Economic Paleontologists and Mineralogists, Tulsa, 583-622.

DUNHAM, R.J. 1962. Classification of carbonate rocks according to depositional texture. *In* Ham,W.E., (ed.): *Classification of Carbonate Rocks: A Symposium,* AAPG Memoir, 1. American Association of Petroleum Geologists, Tulsa, 108-171.

EL-GHALI, M.A.K., MANSURBEG, H., MORAD, S., AL-AASM, I. & AJDANLISKY, G., 2006. Distribution of diagenetic alterations in fluvial and paralic deposits within sequence stratigraphic framework: Evidence from the Petrohan Terrigenous Group and the Svidol Formation, Lower Triassic, NW Bulgaria. *Sedimentary Geology*, 190: 299-321.

GARZANTI, E. & VEZZOLI, G., 2003. A classification of metamorphic grains in sands based on their composition and grade. *Journal of Sedimentary Research*, 73: 830-837.

GIBBONS, K., HELLEN, T., KJEMPERUD, A., NIO, S.D. & VEBBENSTAD, K., 1993. Sequence architecture, facies development and carbonate-cemented horizons in the Troll Field reservoir, offshore Norway. *In* Ashton, M., (ed.), *Advances in reservoir geology*, Geological Society Special publications, 69. Blackwell Scientific Publications, Oxford, 1-31.

GUERIN-FRANIATTE, S. & MULLER, A., 1986. L'Hettangien dans le NE du Bassin de Paris: biostratigraphie et evolution sedimentaire. *Annales de la Société Géologique de Belgique,* 109: 415-429.

GUERIN-FRANIATTE, S., HARY, A. & MULLER, A., 1991. La formation des Grès du Luxembourg, au Lias inférieur: reconstitution dynamique du paléo-environnement. *Bulletin de la Société Géologique de France*, 162: 763-773.

GUILLOCHEAU, F., ROBIN, C., ALLEMAND, P., BOURQUIN, S., BRAULT, N., DROMART, G., FRIEDENBERG, R., GARCIA, J.-P., GAULIER, J.-M. & GAUMET, F. 2000. Meso-Cenozoic geodynamic evolution of the Paris Basin: 3D stratigraphic constraints. *Geodinamica Acta*, 13: 189-245.

HALLAM, A. 2001. A review of the broad pattern of Jurassic sea-level changes and their possible causes in the light of current knowledge. *Palaeogeography Palaeoclimatology Palaeoecology*, 167: 23-37.

HANZO, M., LATHUILIERE, B. & PENIGUEL, G., 1994. The Calcaire-a-Gryphees from Lorraine - a Climate-Induced Limestone Marl Alternation. *Comptes Rendus de l' Academie des Sciences Serie II,* 319: 915-920.

HARTKAMP, C.A., ARRIBAS, J. & TORTOSA, A., 1993. Grain-Size, Composition, Porosity and Permeability Contrasts within Cross-Bedded Sandstones in Tertiary Fluvial Deposits, Central Spain. *Sedimentology*, 40: 787-799.

HARRIS, P.M., KENDALL, C.G.ST.C. & LERCHE, I., 1985. Carbonate cementation - A brief review. In Schneidermann, N. and Harris, P.M., (eds.), *Carbonate cements*, SEPM Special Publication, 36. The Society of Economic Paleontologists and Mineralogists, Tulsa, 79-95.

HARY, A. & MULLER, A. 1993. Trace fossil assemblages and ichnofacies as tools to test the sedimentological model of the Luxembourg Sandstone Formation. (Hettangian/ Sinemurian, NE Paris Basin). *Zentralblatt für Geologie und Paläontologie*, Teil I, 5: 569-587.

HENDRY, J.P., DITCHFIELD, P.W. & MARSHALL, J.D., 1995. Two-stage neomorphism of Jurassic aragonite bivalves: implications for early diagenesis. *Journal of Sedimentary Research*, A65: 214-224.

HENDRY, J.P., WILKINSON, M., FALLICK, A.E. & HASZELDINE, R.S., 2000. Ankerite Cementation in Deeply Buried Jurassic Sandstone Reservoirs of the Central North Sea. *Journal of Sedimentary Research*, 70: 227-239.

JENKYNS, H.C., JONES, C.E., GROCKE, D.R., HESSELBO, S.P. & PARKINSON, D.N., 2002. Chemostratigraphy of the Jurassic System: applications, limitations and implications for palaeoceanography. *Journal of the Geological Society*, 159: 351-378.

JOHNSON, H.D. & BALDWIN, C.T. 1986. Shallow siliciclastic seas. *In* Reading, H.G., (ed.), *Sedimentary Environments and Facies seconded*, Blackwell Scientific Publications, Oxford, 229-282.

KANTOROWICZ, J.D., BRYANT, I.D. & DAWANS, J.M., 1987. Controls on the geometry and distribution of carbonate cements in Jurassic sandstones: Bridport sands, southern England and Viking Group, Troll Field, Norway. *In* Marshall, J.D., (ed), *Diagenesis of sedimentary sequences*, Geological Society Special publications, 36. Blackwell Scientific Publications, Oxford, 103-118.

KETZER, J.M., MORAD, S., EVANS, R. & AL-AASM, I.S., 2002. Distribution of diagenetic alterations in fluvial, deltaic, and shallow marine sandstones within a sequence stratigraphic framework: Evidence from the Mullaghmore Formation (Carboniferous), NW Ireland. *Journal of Sedimentary Research*, 72: 760-774.

LUCIUS, M. 1948. *Erläuterungen zu der geologischen Spezialkarte von Luxemburg - Das Gutland. Veröffentlichtchungen des Luxemburger Geologischen Dienstes*, Band V. Ministère des Travaux Publics, Service Géologique de Luxembourg, Luxembourg, 408 pp.

MARSHALL, J.D. & ASHTON, M., 1980. Isotopic and Trace-Element Evidence for Submarine Lithification of Hardgrounds in the Jurassic of Eastern England. *Sedimentology*, 27: 271-289.

MARSHALL, J.D., 1981. Zoned Calcites in Jurassic Ammonite Chambers - Trace-Elements, Isotopes and Neomorphic Origin. *Sedimentology*, 28: 867-887.

MACHENT, P.G., TAYLOR, K.G., MACQUAKER, J.H.S. & MARSHALL, J.D., 2007. Patterns of early post-depositional and burial cementation in distal shallow-marine sandstones: Upper Cretaceous Kenilworth Member, Book Cliffs, Utah, USA. *Sedimentary Geology*, 198: 125-145.

MALIVA, R.G., MISSIMER, T.M. & DICKSON, J.A.D., 2000. Skeletal aragonite neomorphism in Plio-Pleistocene sandy limestones and sandstones, Hollywood, Florida, USA. Sedimentary Geology, 136: 147-154.

MCBRIDE, E.F., PICARD, M.D. & FOLK, R.L., 1994. Oriented Concretions, Ionian Coast, Italy - Evidence of Groundwater-Flow Direction. *Journal of Sedimentary Research* , A64: 535-540.

MERTENS, G., SPIES, E.-D. & TEYSSEN, T., 1983. The Luxemburg Sandstone Formation (Lias), a tide-controlled deltaic deposit. *Annales de la Société Géologique de Belgique*, 106: 103-109.

MOLENAAR, N., 1990. Calcite Cementation in Shallow Marine Eocene Sandstones and Constraints of Early Diagenesis. *Journal of the Geological Society*, 147: 759-768.

MOLENAAR, N., 1998. Origin of low-permeability calcite-cemented lenses in shallow marine sandstones and CaCO3 cementation mechanisms: an example from the Lower Jurassic Luxemburg Sandstone, Luxemburg. *In* Morad, S., (ed.), *Carbonate cementation in sandstones*, Special publication of the International Association of Sedimentologists, 26. Blackwell Science, Cambridge, 193-211.

MONTEYNE, R., 1967. *Paleogéographie du Bas-Luxembourg au Jurassique inférieur*. Le Pays Gaumais, 27ème-28ème années, 21-41.

MORAD, S., KETZER, J.M. & DE ROS, L.F., 2000. Spatial and temporal distribution of diagenetic alterations in siliciclastic rocks: implications for mass transfer in sedimentary basins. *Sedimentology*, 47: 95-120.

MOZLEY, P.S. & DAVIS, J.M., 1996. Relationship between oriented calcite concretions and permeability correlation structure in an alluvial aquifer, Serra Ladrones Formation, New Mexico. *Journal of Sedimentary Research*, 66: 11-16.

MUCHEZ, P., PEETERS, C., KEPPENS, E. & VIAENE, W.A., 1993. Stable Isotopic Composition of Paleosols in the Lower Visean of Eastern Belgium - Evidence of Evaporation and Soil-Gas CO2. Chemical Geology, 106: 389-396.

NELSON, C.S. & JAMES, N.P., 2000. Marine cements in mid-Tertiary cool-water shelf limestones of New Zealand and southern Australia. *Sedimentology*, 47: 609-629.

PROSSER, D.J., DAWS, J.A., FALLICK, A.E. & WILLIAMS, B.P.J., 1993. Geochemistry and diagenesis of stratabound calcite cement layers within the Rannoch Formation of the Brent Group, Murchison Field, North Viking Graben (northern North Sea). *Sedimentary Geology*, 87: 139-164.

SCHRECK, H., 1976. *Ein Schüttungsmodell des Luxemburger Sandsteins in der Mulde von Weilerbach (Luxemburg): Untersuchung der Schwermineralführung, der Schrägschichtung, des Geröllspektrums und der durch die Faktorenanalyse aufgeschlüsselten Granulometrie des Sandsteins*. PhD dissertation, Rheinisch-Westfälischen Technische Hochschule, Aachen, 168 pp.

SMITH, A.M. & NELSON, C.S., 2003. Effects of early sea-floor processes on the taphonomy of temperate shelf skeletal carbonate deposits. *Earth-Science Reviews,* 63: 1-31.

TAYLOR, K.G., GAWTHORPE, R.L. AND VA&N WAGONER, J.C., 1995. Stratigraphic control on laterally persistent cementation, Book-Cliffs, Utah. *Journal of the Geological Society*, 152: 225-228.

VECSEI, A. & DURINGER, P. 2003. Sequence stratigraphy of Middle Triassic carbonates and terrigenous deposits (Muschelkalk and Lower Keuper) in the SW Germanic Basin: maximum flooding versus maximum depth in intracratonic basins. *Sedimentary Geology*, 160: 81-105.

WALDERHAUG, O., BJØRKUM, P.A. & NORGARD BOLAS, H.M., 1989. Correlation of calcite-cemented layers in shallow-marine sandstones of the Fensfjord Formation in the Brage Field. *In* Collinson, J.D., (ed.), *Correlation in Hydrocarbon Exploration*. Graham and Trotman, London, 367-375.

WALDERHAUG, O. & BJØRKUM, P.A., 1992. Effect of Meteoric Water-Flow on Calcite Cementation in the Middle Jurassic Oseberg Formation, Well 30/3-2, Veslefrikk Field, Norwegian North-Sea. *Marine and Petroleum Geology*, 9: 308-318.

WALDERHAUG, O. & BJØRKUM, P.A., 1998. Calcite cement in shallow marine sandstones: growth mechanisms and geometry. *In* Morad, S., (ed.), *Carbonate cementation in sandstones*, Special publication of the International Association of Sedimentologists, 26. Blackwell Science, Cambridge, 179-192.

WESTPHAL, H. 2006. Limestone-marl alternations as environmental archives and the role of early diagenesis: a critical review. *International Journal of Earth Sciences*, 95: 947-961.

WILKINSON, B.H., SMITH, A.L. & LOHMANN, K.C., 1985. Sparry calcite marine cement in upper Jurassic limestones of southeastern Wyoming. *In* Schneidermann, N. and Harris, P.M., (eds), *Carbonate cements*, SEPM Special Publication, 36. The Society of Economic Paleontologists and Mineralogists, Tulsa, 169-184.

WILKINSON, M., 1991. The Concretions of the Bearreraig Sandstone Formation - Geometry and Geochemistry. *Sedimentology*, 38: 899-912.

WILKINSON, M., 1993. Concretions of the Valtos Sandstone Formation of Skye - Geochemical Indicators of Palaeo-Hydrology. *Journal of the Geological Society*, 150: 57-66.

WILSON, P.A. & DICKSON, J.A.D., 1996. Radiaxial calcite: Alteration product of and petrographic proxy for magnesian calcite marine cement. *Geology*, 24: 945-948.

(Manuscript received 17.10.2007, accepted 20.05.2008, published on line 01.07.2008)

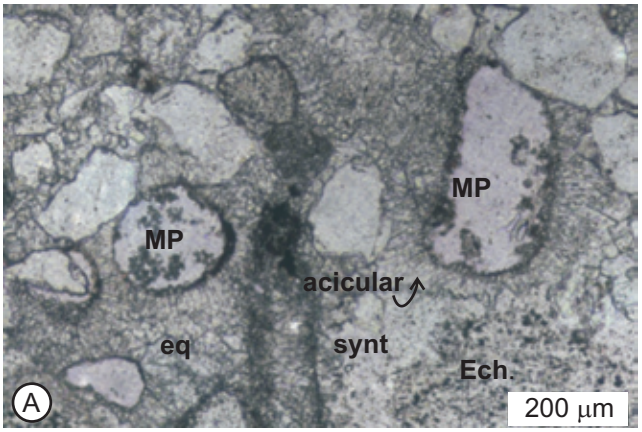
MP
MP
acicular
eq
synt
Ech.
A
200 µm

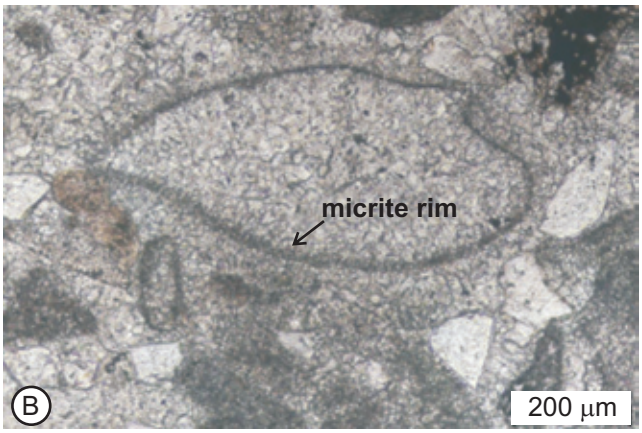
micrite rim
B
200 µm

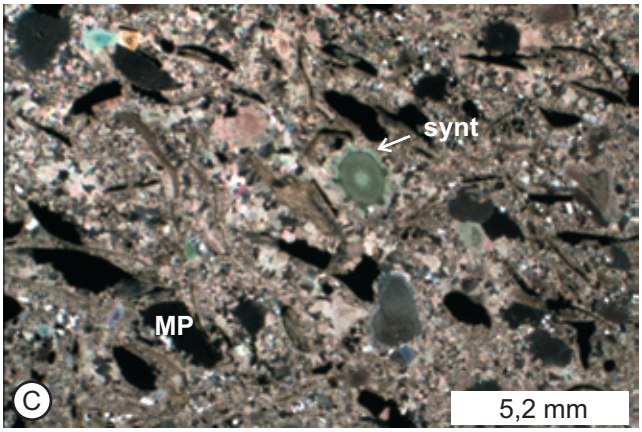
synt
MP
C
5,2 mm

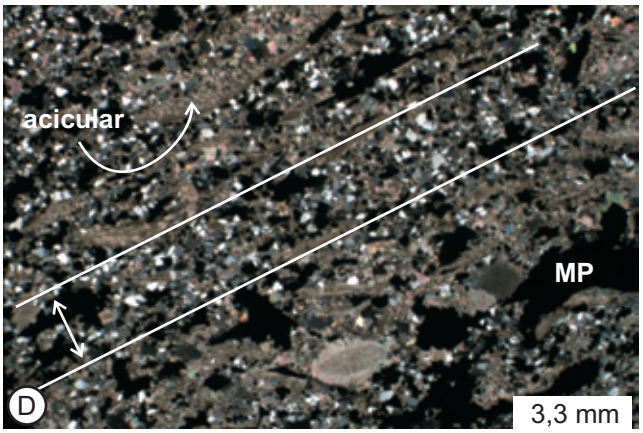
acicular
MP
D
3,3 mm

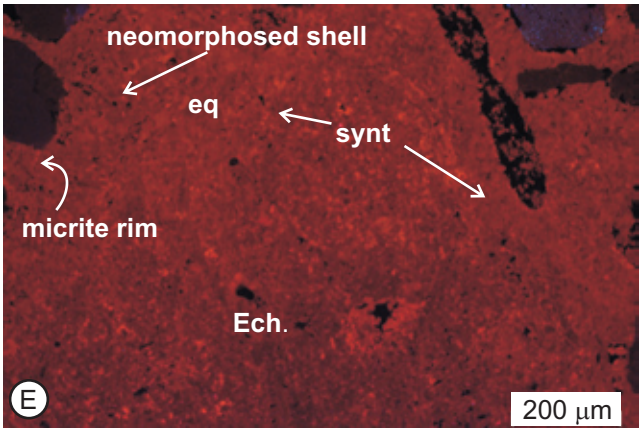
neomorphosed shell
eq
synt
micrite rim
Ech.
E
200 µm

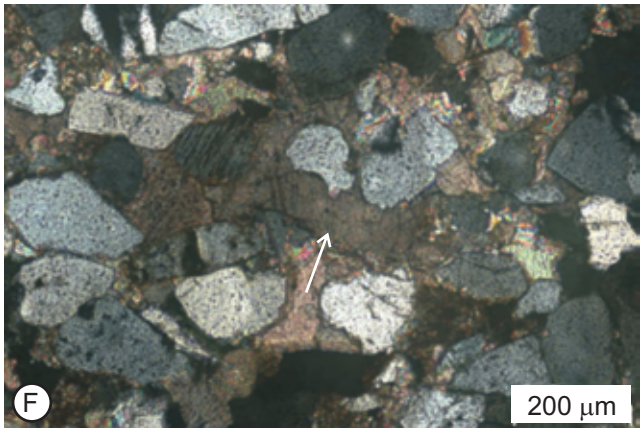
F
200 µm

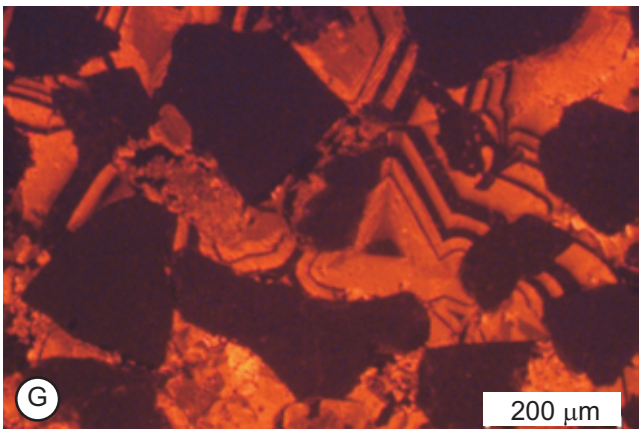
G
200 µm

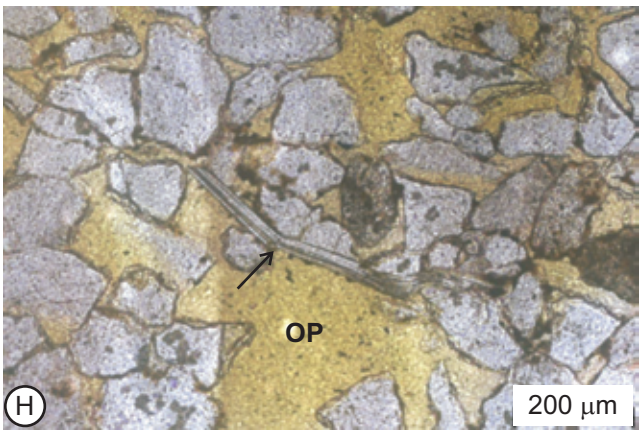
OP
H
200 µm

Plate 1. Microphotographs in plane or cross polarized light (PPL and XPL respectively), or cathodoluminescence (CL) of: (A) Well developed acicular cements on recrystallised carbonate particles and moldic pores (MP) as well as syntaxial overgrowths (synt) on an echinoderm fragment (Ech). Equant cements (eq.) fill up the remaining primary porosity and recrystallised carbonate fragments (PPL). (B) Recrystallised bivalve, whose outline has been preserved by the micrite envelope. The outline of the acicular cement fringe can be recognised on the micrite rim (PPL). (C) Cementation within coarse grained, bioclast rich foreset laminae. Syntaxial (synt) overgrowths on echinoderm fragment are well developed. Most of bivalve fragments retained their original structure. In de lower part of the microphotograph some moldic porosity (MP) is visible. (XPL) (D) Relationship between the composition and grain size in coarse-grained layers. The zone between the white lines is a finer grained quartz rich foreset lamina. (E) Echinoderm (ech), syntaxial overgrowth (synt) and equant (eq) cements filling up primary pores and replacing a shell fragment, all expose the same type of dull red to orange luminescence (CL). (F) Late syntaxial to poikilotopic cements (arrow) in a small nodular cemented lens (XPL). (G). Non-bright multiple zoned calcite cements of the cemented pebble (CL). (H) Broken mica flake (arrow) in a compacted uncemented sand and presence of oversized pore (OP) (PPL).

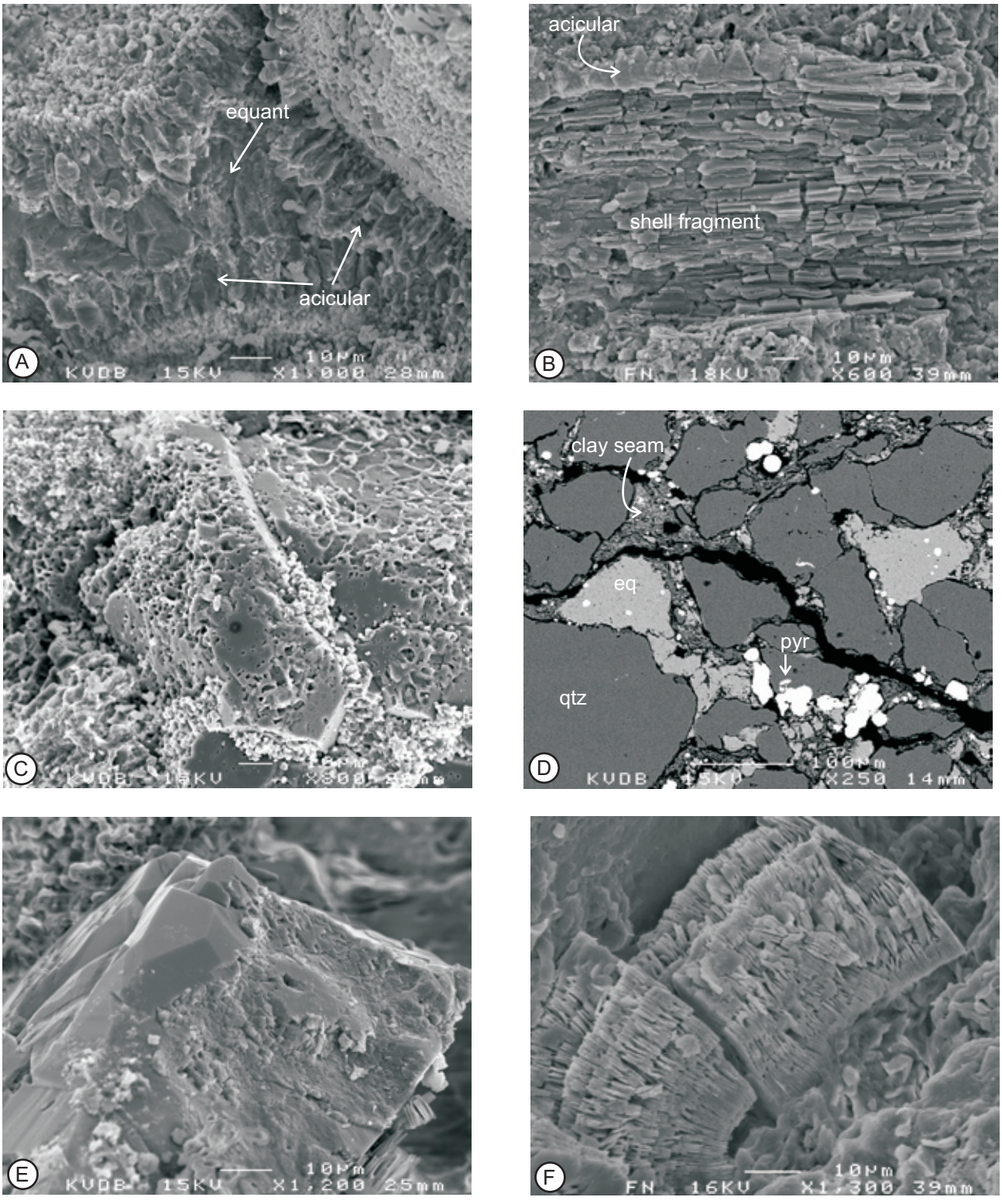

Plate 2. Secondary electron (SEM-SE) and Backscatter (SEM-BSE) microphotographs from broken rock fragments (not etched) and thin sections respectively: (A) Acicular and equant cements in an oolitic sandstone (SEM). (B) Small acicular cements on a shell fragment in a very fine grained sand (SEM). (C) Corrosion textures on quartz grains and authigenic quartz overgrowths. (SEM) (D) Occurrence of pyrite in a clay seams of a very fine grained sandstone. qtz: quartz, eq: equant cement, pyr: pyrite. This sample occurs along the edge of a cemented lens. (BSE). (E) Quartz cements on grains in the uncemented interval above a cemented lens. The irregular corrosion on the surface implies that calcite cements might have been present. Notice the presence of small kaolinite booklets in the right lower corner (SEM) (F) Kaolinite booklet structure (SEM).